# Recent Research Topics in My Work Related to ML and DL

- Deep learning-based surrogate models for flood map prediction
- Streamflow forecasting using deep learning techniques
- Calibration of distributed hydrological models with machine learning techniques

# INTEGRATING NET RAINFALL CALCULATION IN DEEP LEARNING-BASED SURROGATE MODELING FRAMEWORKS FOR URBAN FLOOD PREDICTION

Juan F. Farfán-Durán[1] Luis Cea[1], Carlos Montalvo[1], Jerónimo Puertas[1] [1], Joao P. Leitao[2]

*[1]Universidade da Coruña, Water and Environmental Engineering Group, Center for Technological Innovation in Construction and Civil Engineering (CITEEC), A Coruña, Spain*

*[2]Department of Urban Water Management, Swiss Federal Institute of Aquatic Science and Technology (Eawag), Dübendorf, Switzerland*

# Introduction

- 2D and 1D models accurately identify flood risk and water depth maps.
- Studies focus on complex flood effects, interactions.
- High-resolution models need dense meshes, are computationally expensive.
- Their cost limits use in emergency early warning systems.
- **Previously calibrated parameters.**
- Our research uses surrogate Deep Learning (DL) models to speed up the generation of water depth maps.
- The surrogate model is trained with outputs of the costly model to emulate it.

# Study Area Overview

- Location: Coastal Sada, NW Spain, 0.6 km².
- Identified as high flood risk area (APSFR).
- Confluence of *Rego Maior* and *Regato de Fontoira*.
- Culvert box at confluence impacts river and sea interaction.
- Basin size: 24.75 km².
- Main runoff: Urban and industrial areas.
- Combined sewer system with 11 km network
- Recent floods: March 2016, December 2022.

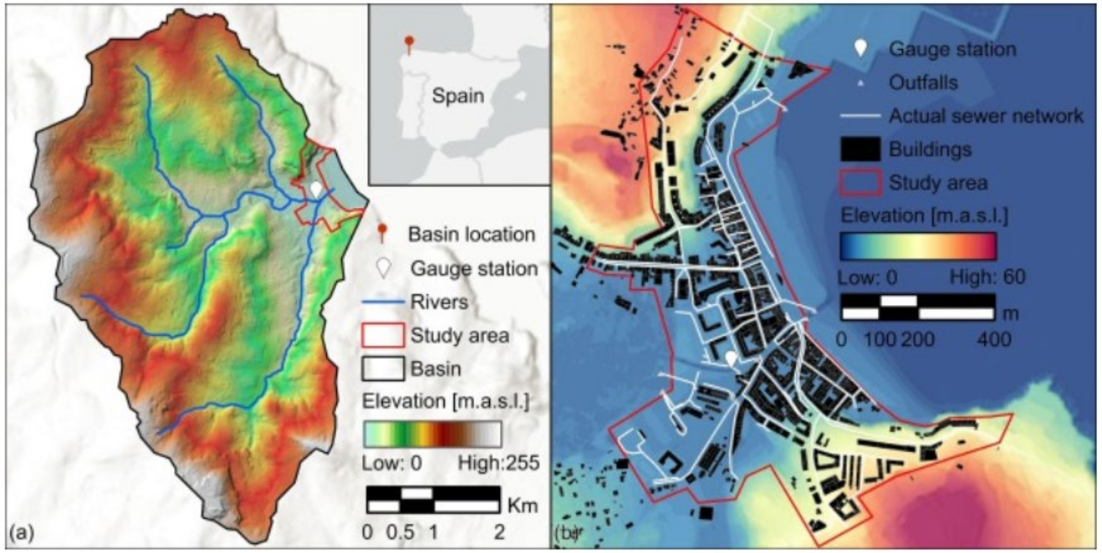

# Overview of Iber-SWMM

- Unstructured mesh with 467,162 elements.
- Varied resolution: hillslopes (30m), coastal/industrial (10m), urban/water streams (2m-1m).
- Sea level as boundary condition, constant for synthetic events.
- Simplified Manning coefficients for roughness.

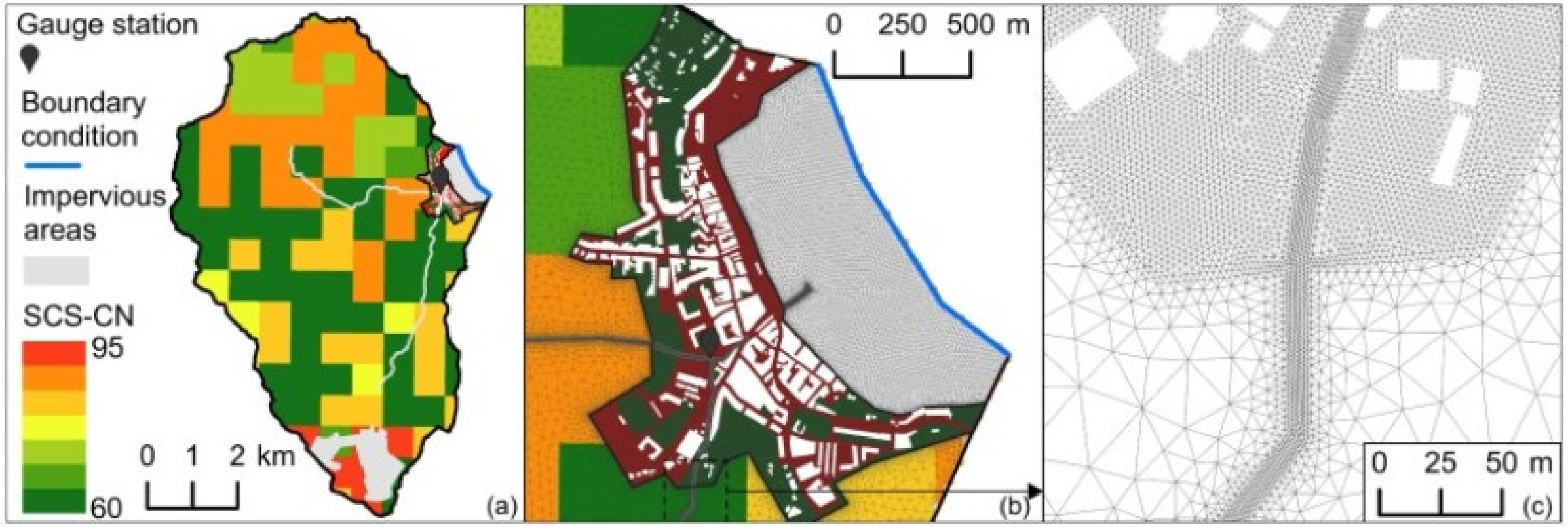

# Overview of Iber-SWMM

- Combination of 1D and 2D models.
- Simulates surface and sewer flow dynamics.
- Used for detailed flood event analysis.
- 2D free-surface flow simulation.
- 1D dynamic sewer network model.
- Synchronized water exchange maintains mass balance.
- Interaction through inlets and manholes.

# Data: Terrain Features

- Elevation: Altitude representation (25m resolution).
- Slope: Steepness of the terrain.
- Aspect: Shows the slope direction.
- Curvature: Terrains convexity or concavity (hard to plot).
- Mask: Displays excluded or included areas.
- Stream Power Index: Erosive potential of watercourses based on slope.
- Curve Number (SCS-CN): Grid with varying values related to runoff estimation.

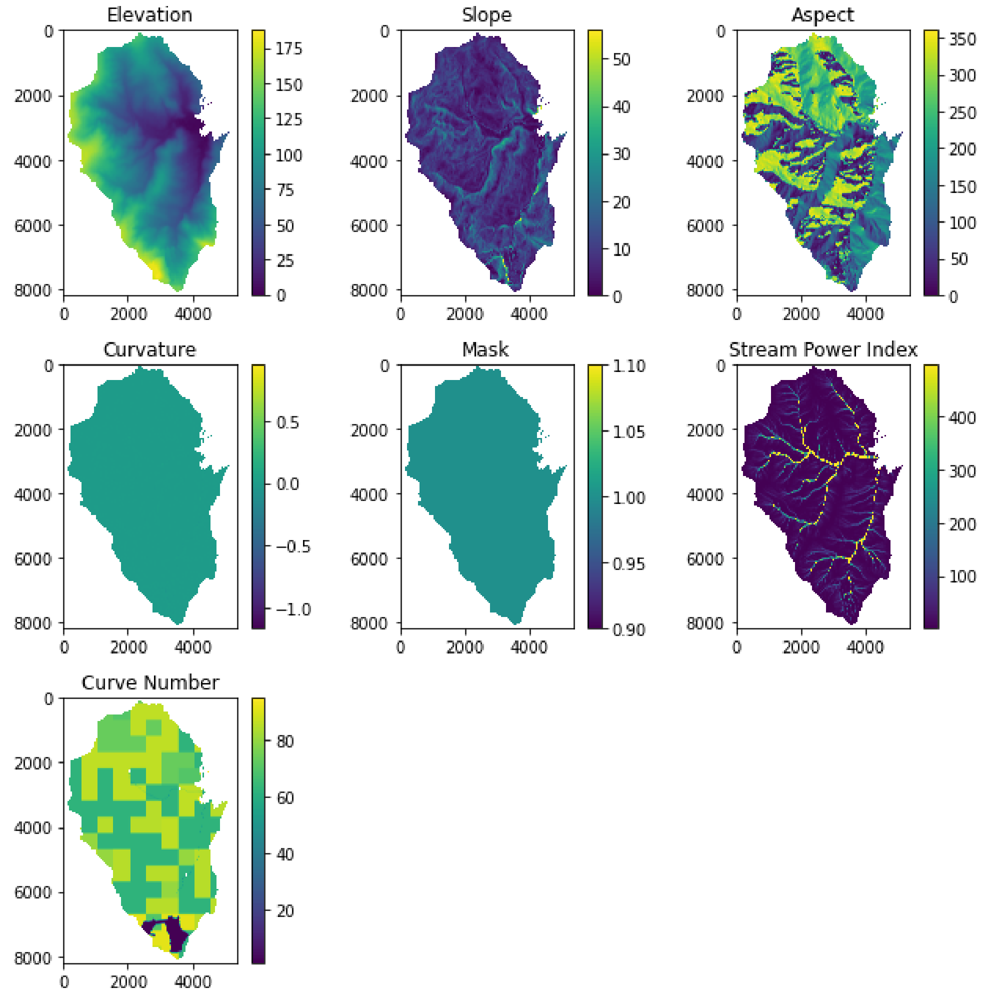

# Data: Rain Patterns

- Time series: 120 steps, hourly scale.
- Precipitation from raster images.
- Iber runs with the images; surrogate uses averaged series.
- Synthetic tide series incorporated for compound effects.

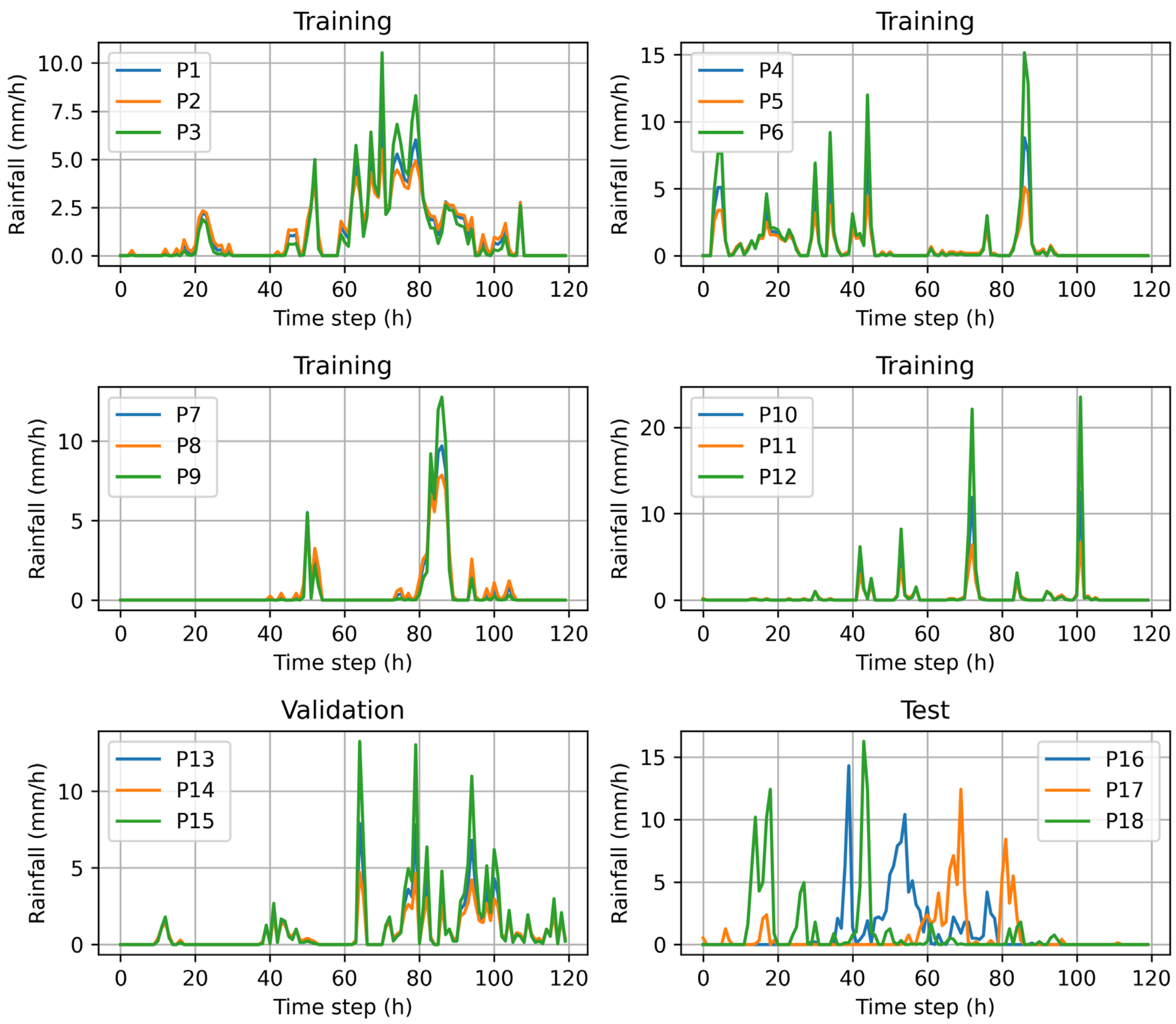

# Data: Water depth Maps

- The events were then modeled in Iber-SWMM.
- Maps capture maximum water depths in 120 time steps.
- Examples provided for various precipitation intensities.
- Current map computation: ~3 hours (**After Calibration)**

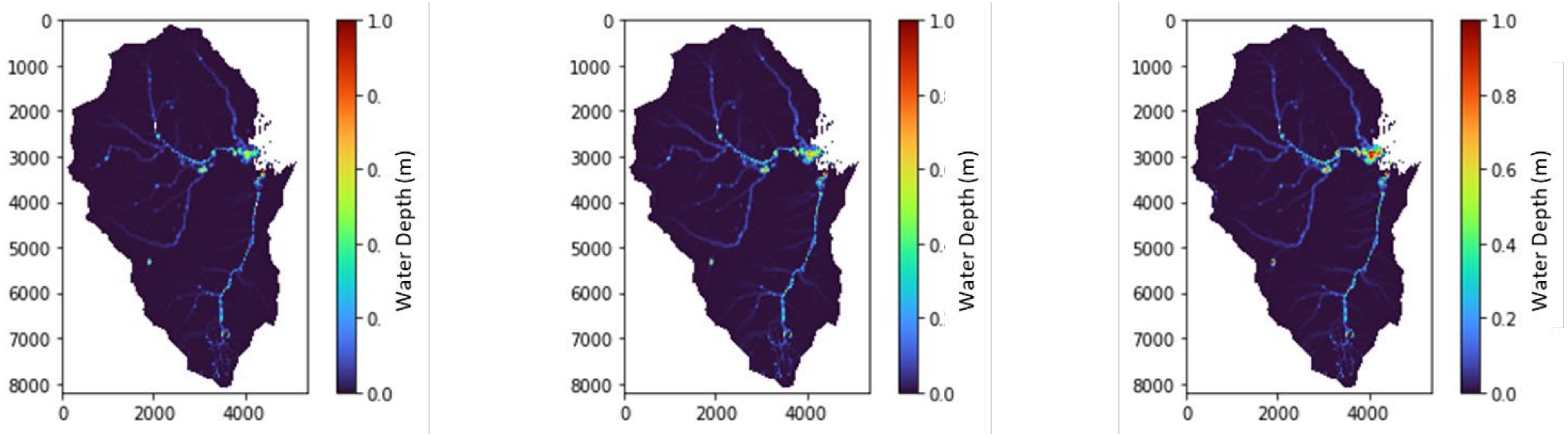

# U-Net: Spatial Variability of Infiltration

- Originally designed for biomedical image segmentation.
- Features a contracting path for context and an expanding path for precise localization.
- Efficient with small data sets due to data augmentation capabilities.
- Adaptable to applications beyond medical imaging, like satellite imagery, autonomous driving and wader depth prediction.

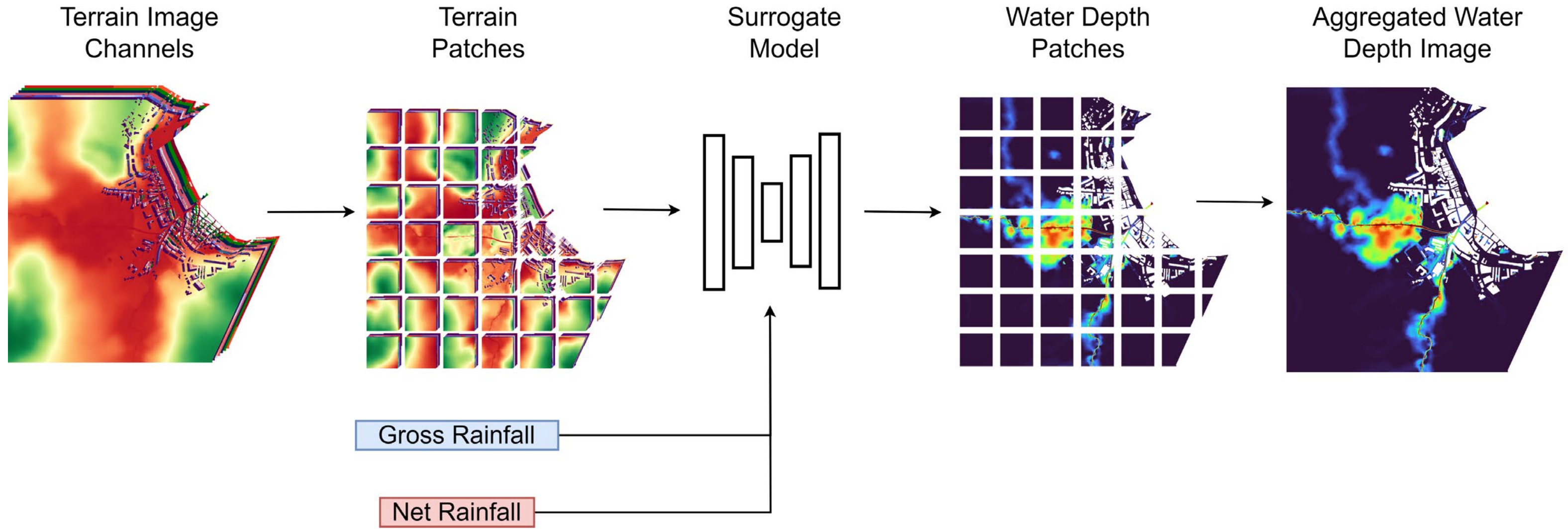

# U-Net: Spatial Variability of Infiltration

### U-Net

- Different architectures have been tested, this one is the best one so far.
- The main characteristic is the inclusion of three inputs: terrain patch, gross rainfall, and net rainfall.

### Gross and Net Rainfall Calculations

- Gross rainfall is uniform across all patches.
- Net rainfall is dynamically calculated for each patch, considering the spatial variability of infiltration.

### Terrain Patch Analysis

- Average CN for each patch is calculated from the terrain image data.
- This CN is used to estimate the field capacity (S) at the beginning of the event.

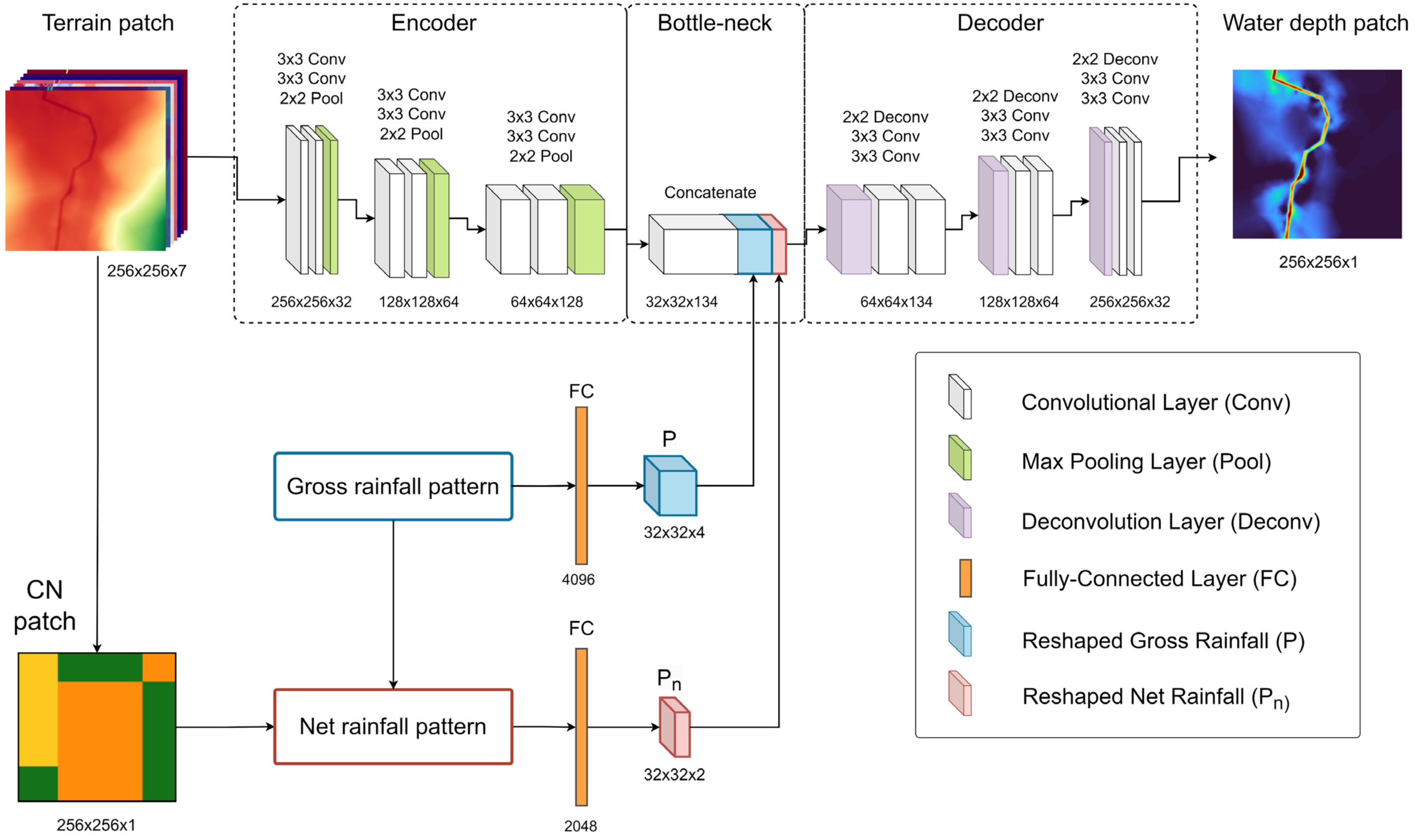

# U-Net: Spatial Variability of Infiltration

### Adjustments for Moisture Conditions

- IBER includes a "multiplier" parameter to adjust the CN image uniformly, reflecting different antecedent moisture conditions.
- Net rainfall is computed dynamically in the training pase.
- This adjustment allows the model to map flood scenarios under varying soil moisture conditions.

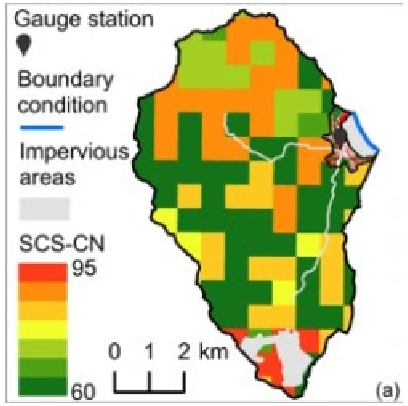


**X** *(multiplier)*

***(0.3, 0.5, 0.7, 1)***

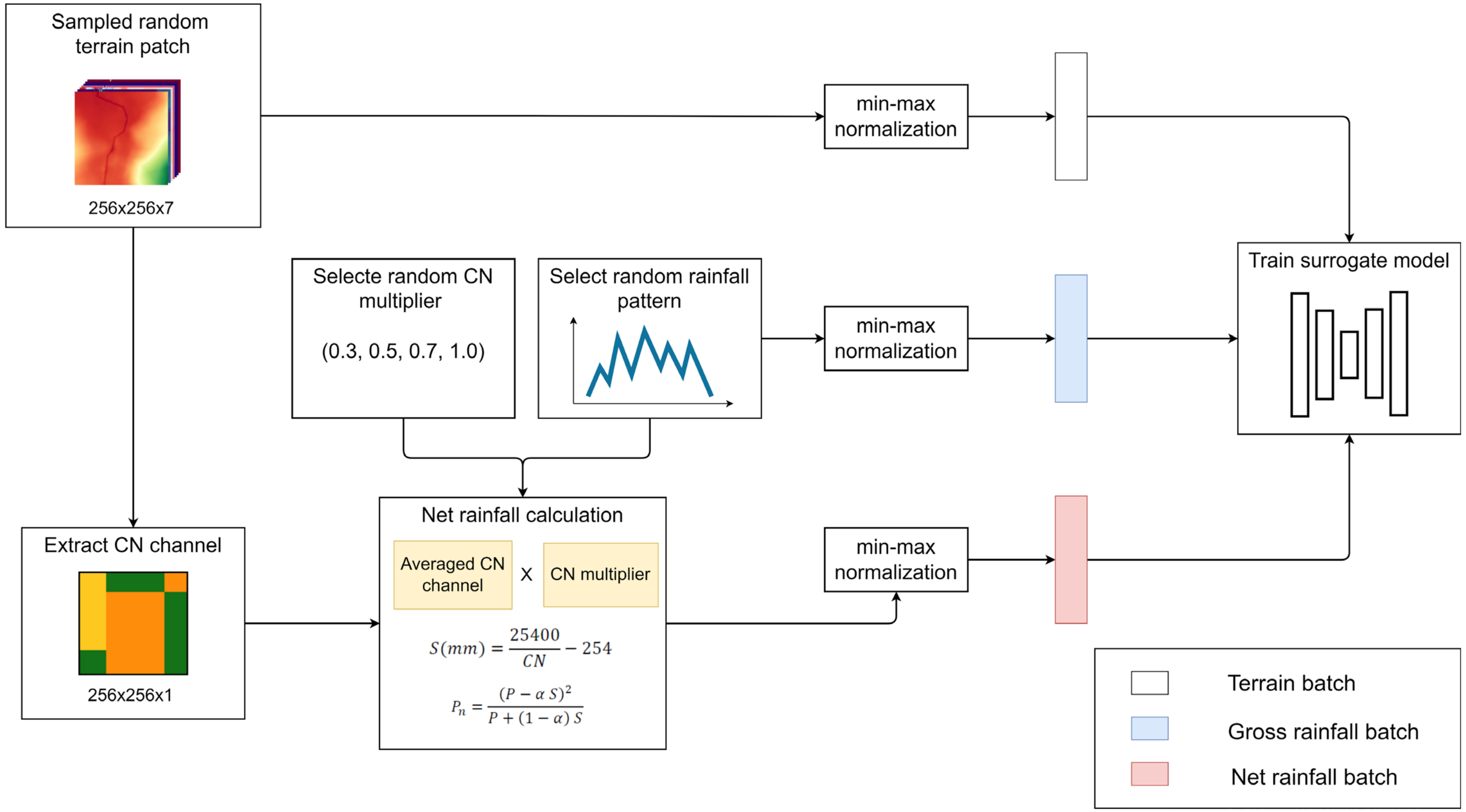

# U-Net: Spatial Variability of Infiltration

## Model Training and Execution

- The surrogate model incorporates these multipliers and has been trained accordingly.
- Net rainfall for each patch is computed before processing by the model.
- The model requires about 3-4 hours for training, enabling **dynamic training** that accounts for these calculations.
- Once trained, the generation of a water depth map takes about 3 seconds
- Loss values decrease indicating convergence.

# U-Net: Spatial Variability of Infiltration

## Model Training and Validation

- The model has been trained and validated using observed and perturbed data sets.
- A real event from December 2022 was reserved and never shown to the neural network during any stage of training.
- The multiplier for CN is 0.5 (this event has evaluated in previous studies, we can use that for analysis).

## Demonstration of Model Prediction

- The model's prediction capabilities are showcased using the event from December 2022.
- A specific prediction patch from this event is displayed to illustrate the model's performance.

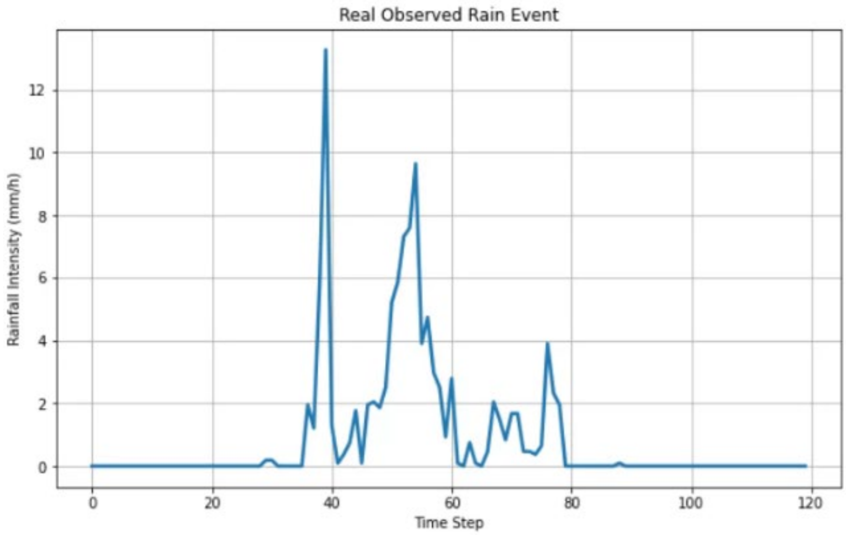


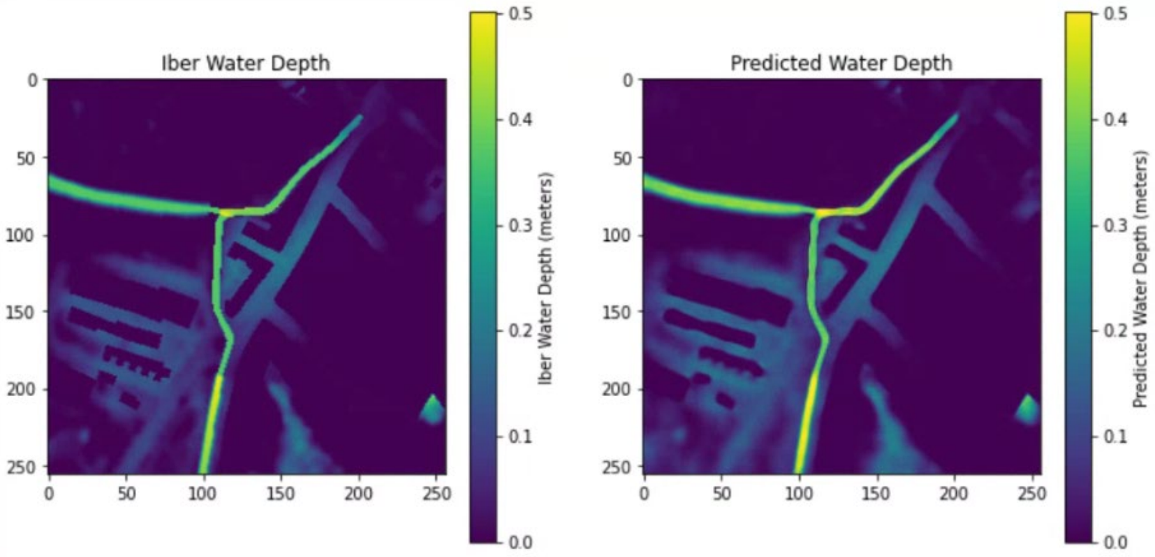

# U-Net: Spatial Variability of Infiltration

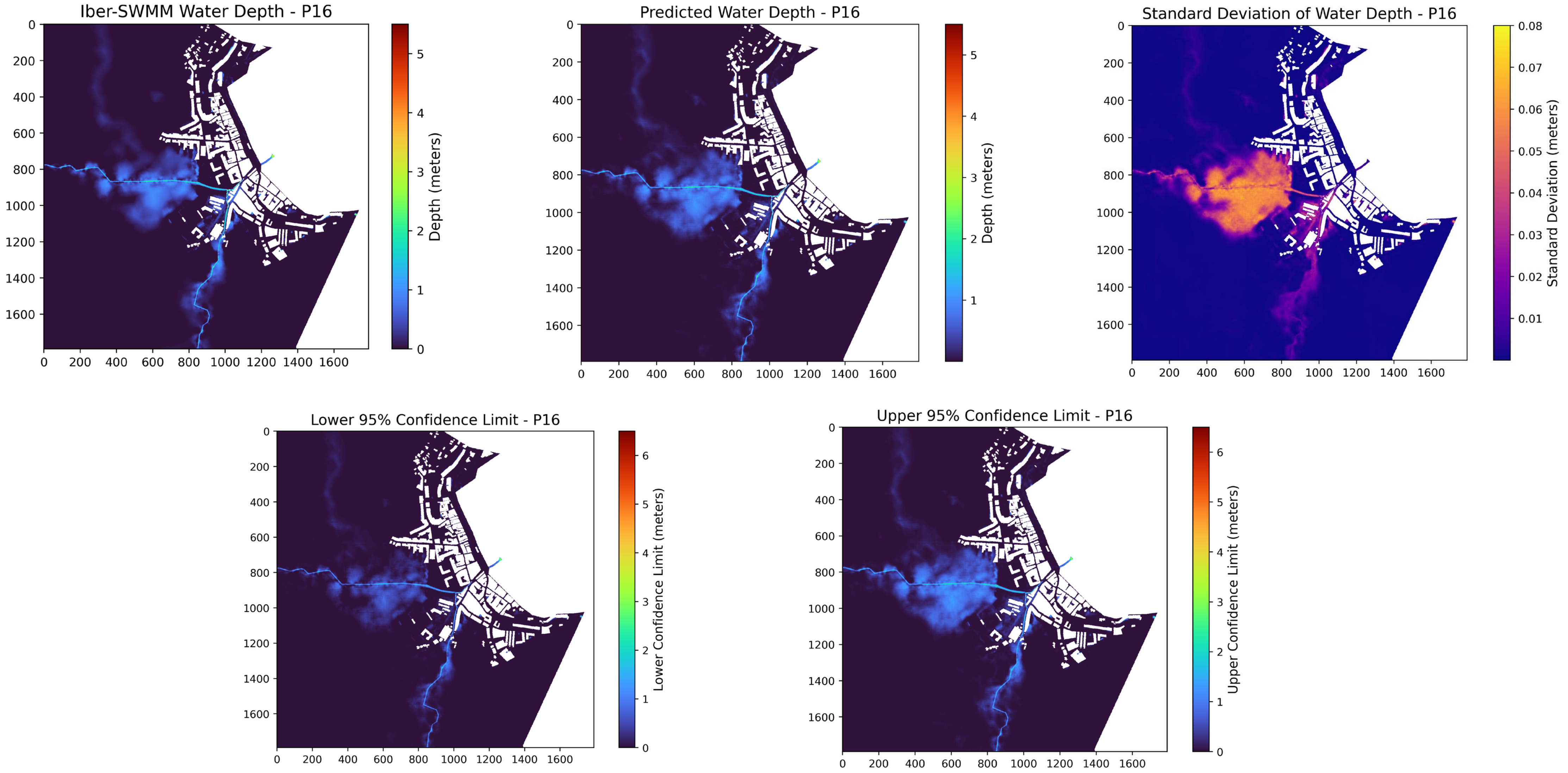

# U-Net: Spatial Variability of Infiltration

- **Presentation of Model Outputs**
  - The images display the maximum water depth maps for the selected event.
  - A second image is shown, which has been filtered using a mask to only include pixels with water depths greater than 10 centimeters.
  - The primary concern being addressed is the depth of flooding, highlighting where the model needs further refinement or validation.

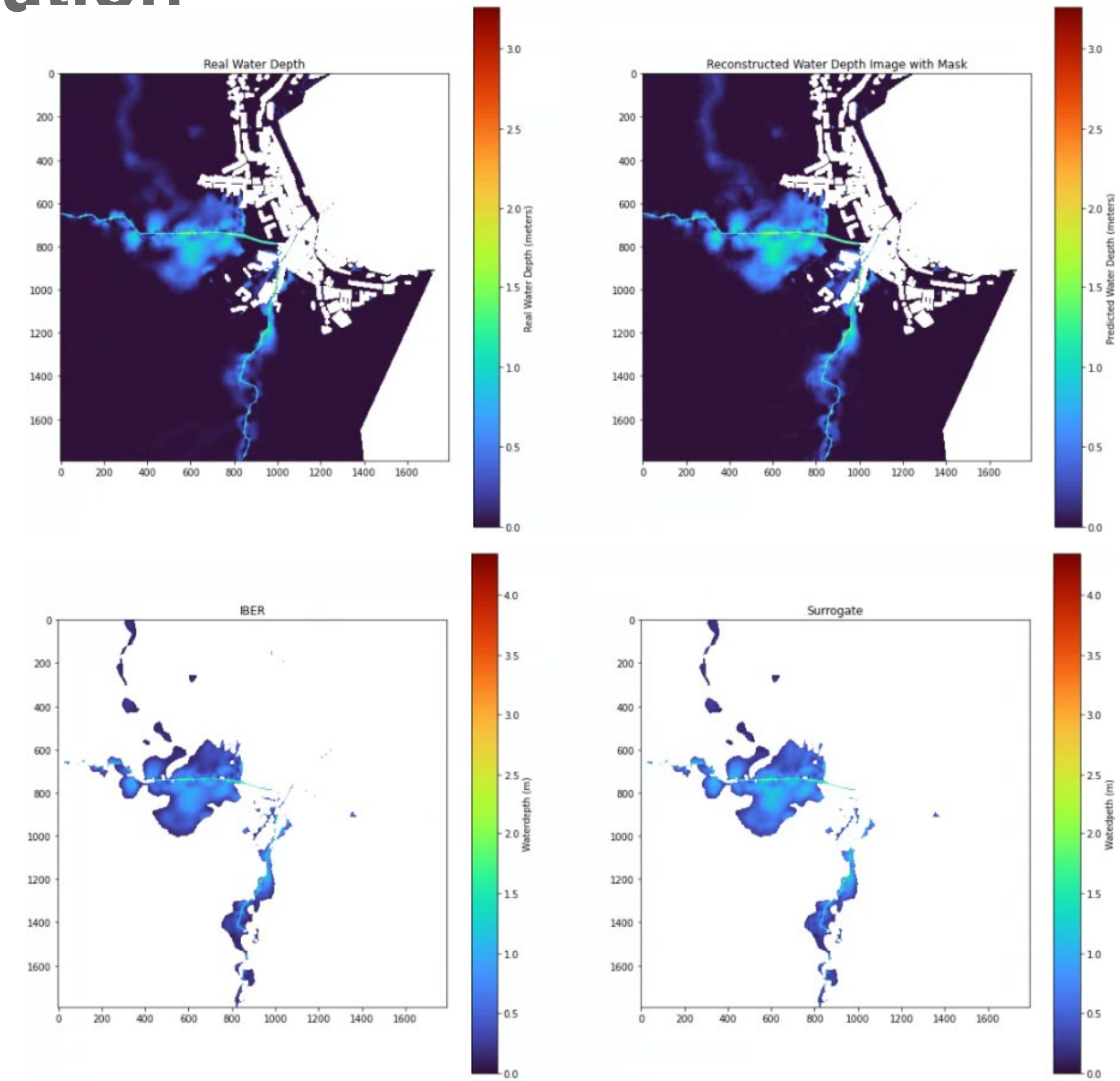

# U-Net: Spatial Variability of Infiltration

**Observations on Water Depth**

- There is a noticeable bias in pixels showing greater depths, specifically around 20-30 centimeters.
- Low dispersion in the results suggests that the neural network architecture is effective and consistent.

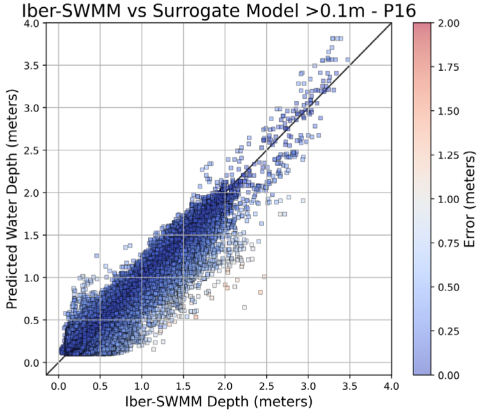


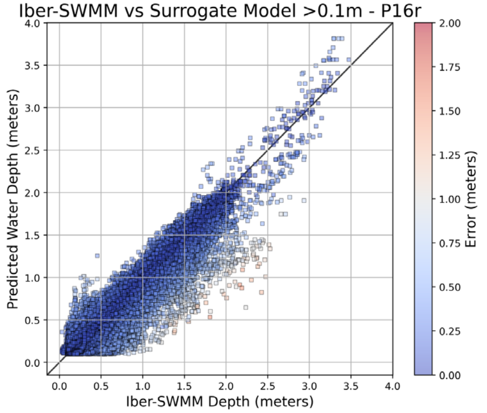


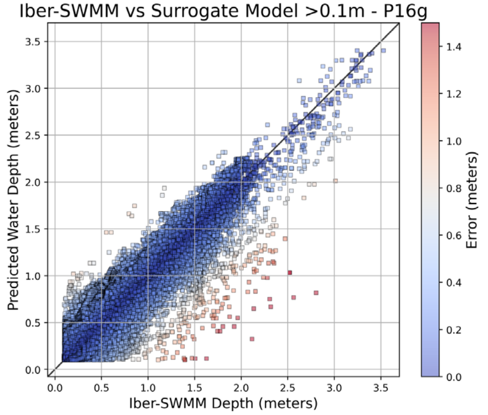


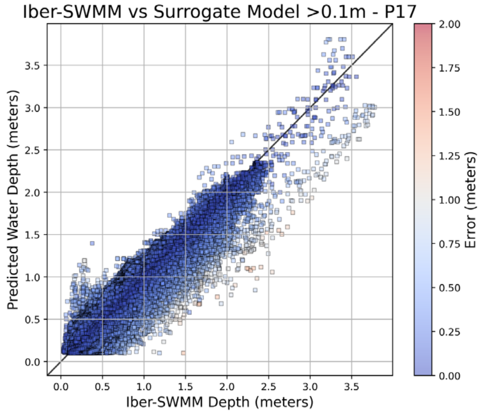


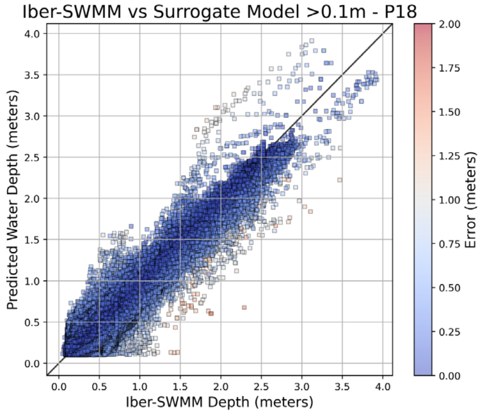

# Flood extension

- Two analyses: complete area and urban focus.
- High HR for complete area, satisfactory performance.
- Slight HR decrease in urban area analysis.
- SM1 closely matches Iber-SWMM flood extents.
- Challenges in extrapolating extreme flood scenarios.
- Broader confidence intervals for less extreme events.
- No significant difference: averaged vs raster inputs.

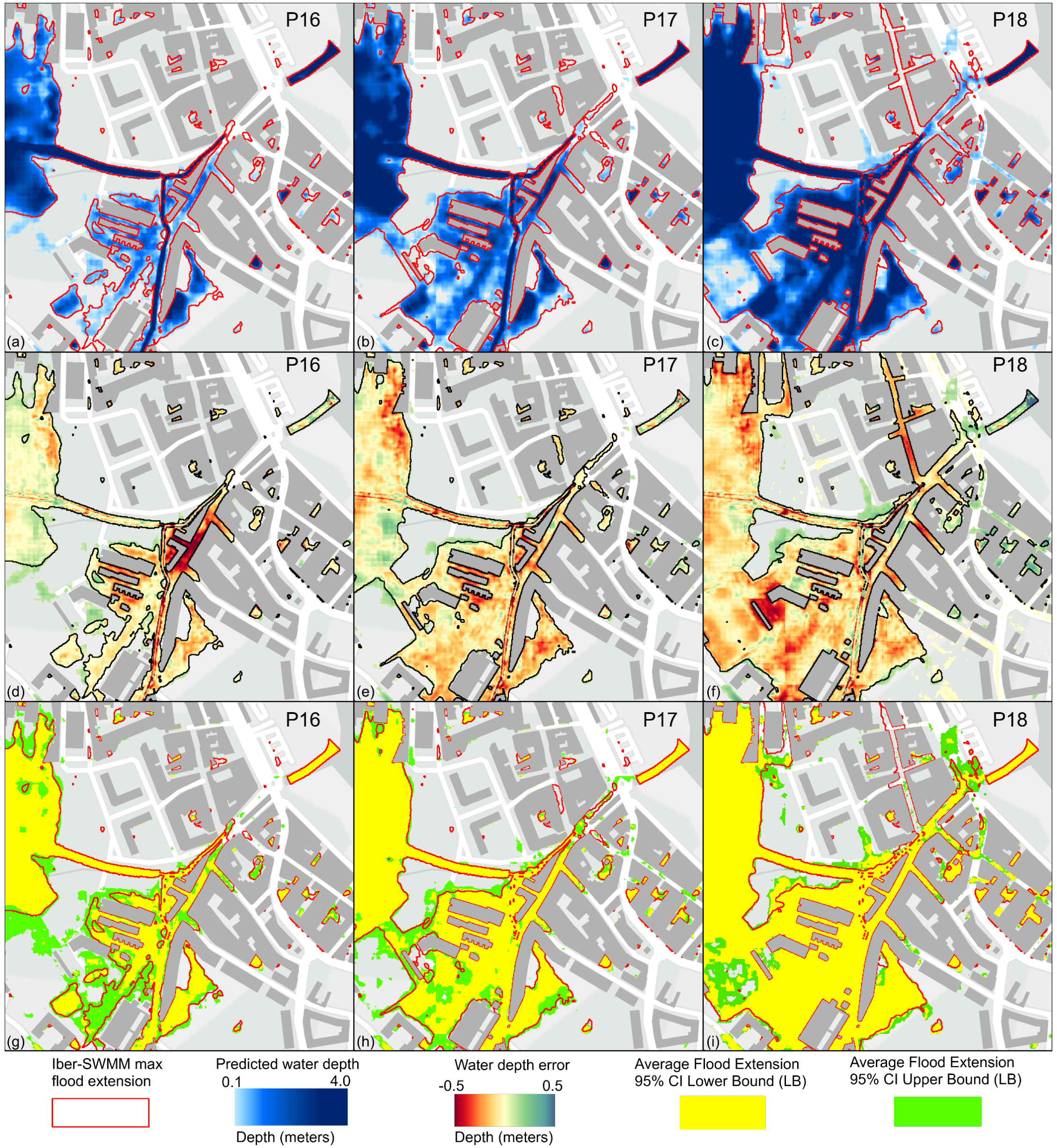

# Conclusions

**Conclusions**

- Current architecture predicts flood maps with acceptable precision.
- Calculation time for December 2022 event in Iber is about 3 hours.
- With the surrogate, calculation time reduces to about 3 seconds (without uncertainty).

**Adjustment of Multiplier Ranges**

- Modify the range of CN multipliers to prevent the model from needing to extrapolate, and evaluate the impact on results.

**Model for Uncertainty Estimation**

- Develop a model capable of calculating maps for different multipliers and estimating maps with uncertainties to better handle variable conditions.

# A COMPARATIVE ANALYSIS OF DEEP LEARNING TECHNIQUES FOR RIVER FLOW FORECASTING IN NORTHWEST SPAIN

Juan F. Farfán-Durán, Luis Cea

Universidade da Coruña, Water and Environmental Engineering Group, Center for Technological Innovation in Construction and Civil Engineering (CITEEC), Elviña, 15071 A~Coruña, Spain

# Introduction

- Streamflow prediction important for water resource management
- Hydroelectric efficiency and irrigation planning
- Reservoir operations and flood management
- Challenges due to non-linear streamflow nature
- Complexity from weather, terrain, and human activities
- Hydrological models simulate watershed responses
- Two main types: physically-based and data-driven
- Deep learning (DL) captures extensive data patterns

# Objectives

- Evaluate DL models for hourly streamflow prediction (first aproximation)
- DL models:
  - **LSTM**: Long Short-Term Memory
  - **GRU**: Gated Recurrent Units
  - **CNN**: Convolutional Neural Network
  - **Hybrid CNN Models**: Models that combine features of CNNs with other types of neural networks
- Focus on two different-sized basins in Northwest Spain
- DL models are applied in various lead times
- Monte Carlo Dropout (MCD) for uncertainty assessment

# Study Area: Groba basin

- Study Area: Groba and Anllóns rivers, NW Spain
- Groba Basin: 17.05 km², complex topography
- Groba elevation range: 35 to 627 m.a.s.l.
- Groba average slope: 27.4%, steep terrain
- 9 meteorological stations in Groba

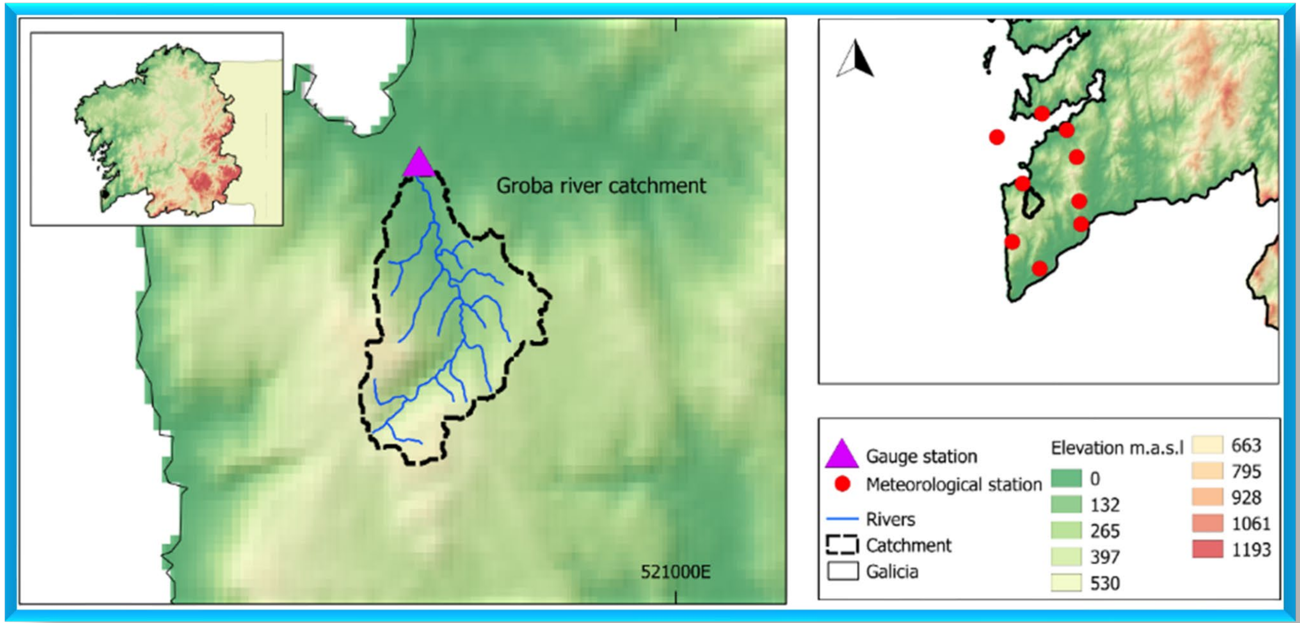

# Study Area: Anllóns basin

- Anllóns basin: 438 km², varied topography
- Anllóns elevation range: 59 to 473 m.a.s.l.
- Anllóns average slope: 12.1%, moderate terrain
- 16 meteorological stations Anllóns

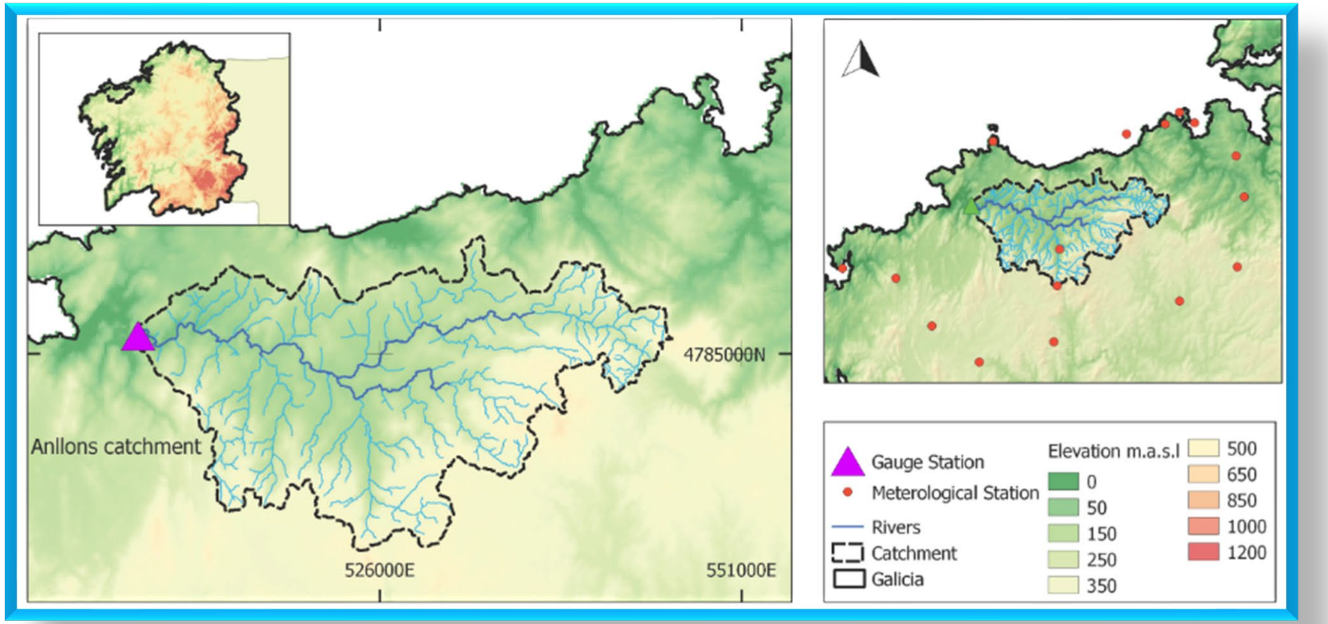

# Data

- December 2008 to September 2018, covering a period of approximately 10 years.
- 80% Training and Cross-Validation
- 20% Reserved for Model Testing

| Groba | | | | | | | | | |
|---|---|---|---|---|---|---|---|---|---|
| Variable | Data count | Mean | Std | P min | P 25% | P 50% | P 75% | P max | Dataset |
| Rainfall (mm/h) | 54661 | 0.15 | 0.69 | 0 | 0 | 0 | 0 | 37.7 | Training |
| | 11016 | 0.14 | 0.61 | 0 | 0 | 0 | 0 | 17.95 | Validation |
| | 17562 | 0.13 | 0.61 | 0 | 0 | 0 | 0 | 8.45 | Test |
| Streamflow ($m^3/s$) | 54661 | 0.74 | 1.05 | 0.03 | 0.13 | 0.42 | 0.93 | 7.96 | Training |
| | 11016 | 0.71 | 0.95 | 0.02 | 0.09 | 0.31 | 0.76 | 6.68 | Validation |
| | 17562 | 0.44 | 0.63 | 0.02 | 0.06 | 0.21 | 0.56 | 7.66 | Test |

*Statistical description of rainfall (mm/h) and streamflow ($m^3/s$) data in the Groba Basin.*

| Anllóns | | | | | | | | | |
|---|---|---|---|---|---|---|---|---|---|
| Variable | Data count | Mean | Std | P min | P 25% | P 50% | P 75% | P max | Dataset |
| Rainfall (mm/h) | 54664 | 0.16 | 0.55 | 0 | 0 | 0 | 0.05 | 15.4 | Training |
| | 13666 | 0.16 | 0.56 | 0 | 0 | 0.03 | 0.08 | 8.57 | Validation |
| | 17562 | 0.14 | 0.53 | 0 | 0 | 0 | 0.03 | 11.29 | Test |
| Streamflow ($m^3/s$) | 54664 | 12.75 | 14.69 | 1.57 | 2.62 | 7.96 | 17.98 | 98.21 | Training |
| | 13666 | 13.94 | 16.25 | 1.45 | 2.56 | 7.35 | 17.49 | 79.11 | Validation |
| | 17562 | 7.92 | 9.99 | 0.9 | 2.25 | 3.93 | 9.45 | 74.19 | Test |

*Statistical description of rainfall (mm/h) and streamflow ($m^3/s$) data in the Anllóns Basin.*

# Data

- December 2008 to September 2018, covering a period of approximately 10 years.
- 80% Training and Cross-Validation
- 20% Reserved for Model Testing

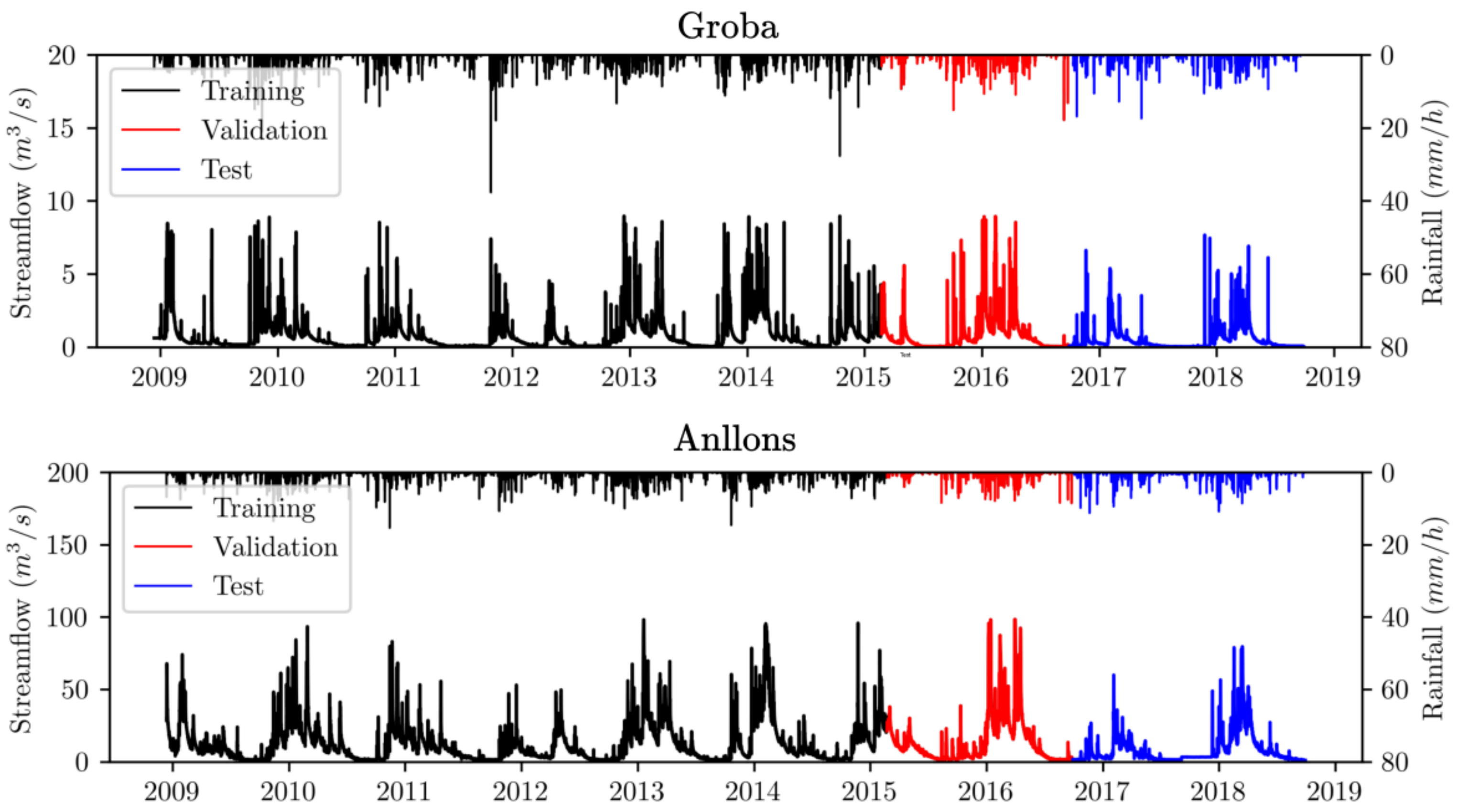

# Methods: DL Models

**Recurrent Neural Networks (RNNs)**

- Structure: Input, hdden, output layers
- Unique feature: Recurrent connections
- Function: Maintains memory across time steps
- Equations: Manage states, inputs, and outputs
- Weights: **W, U, V,** define connections
- Activations: σ and Φ functions

$$\boldsymbol{h}_t = \sigma(\mathbf{W} \cdot \boldsymbol{h}_{t-1} + \mathbf{U} \cdot \boldsymbol{x}_t + \boldsymbol{b}_h)$$
$$\boldsymbol{o}_t = \phi(\mathbf{V} \cdot \boldsymbol{h}_t + \boldsymbol{b}_y)$$

**Long Short-Term Memory (LSTM)**

- LSTM: Overcomes gradient issues in RNNs
- Capable of learning Long-Term dependencies
- Features three gates: Forget (***f***), input (***i***), output (***o***)
- Maintains two states: Cell (***c***) and hidden (***t***)
- Equations govern gate operations and states

$$\boldsymbol{f}_t = \sigma(\mathbf{U}_f \cdot \boldsymbol{x}_t + \mathbf{W}_f \cdot \boldsymbol{h}_{t-1} + \boldsymbol{b}_f)$$
$$\boldsymbol{i}_t = \sigma(\mathbf{U}_i \cdot \boldsymbol{x}_t + \mathbf{W}_i \cdot \boldsymbol{h}_{t-1} + \boldsymbol{b}_i)$$
$$\boldsymbol{o}_t = \sigma(\mathbf{U}_o \cdot \boldsymbol{x}_t + \mathbf{W}_o \cdot \boldsymbol{h}_{t-1} + \boldsymbol{b}_o)$$
$$\boldsymbol{c}_t = \boldsymbol{f}_t \otimes \boldsymbol{c}_{t-1} + \boldsymbol{i}_t \otimes \tanh(\mathbf{U}_c \cdot \boldsymbol{x}_t + \mathbf{W}_c \cdot \boldsymbol{h}_{t-1} + \boldsymbol{b}_c)$$
$$\boldsymbol{h}_t = \boldsymbol{o}_t \otimes \tanh(\boldsymbol{c}_t)$$

# Methods: DL Models

**Gated Recurrent Unit (GRU)**

- GRUs: Advanced RNNs with gating mechanisms
- Designed to manage long temporal sequences
- Features two gates: update ($z$) and reset ($r$)
- Equations manage information flow through gates
- Retains relevant information in long sequences
- Addresses RNN shortcomings like vanishing gradient

$$\boldsymbol{z}_t = \sigma(\mathbf{U_z} \cdot \boldsymbol{x}_t + \mathbf{W_z} \cdot \boldsymbol{h}_{t-1} + \boldsymbol{b}_z)$$
$$\boldsymbol{r}_t = \sigma(\mathbf{U_r} \cdot \boldsymbol{x}_t + \mathbf{W_r} \cdot \boldsymbol{h}_{t-1} + \boldsymbol{b}_r)$$
$$\tilde{\boldsymbol{h}}_t = \tanh(\mathbf{U} \cdot \boldsymbol{x}_t + \boldsymbol{r}_t \otimes \mathbf{W} \cdot \boldsymbol{h}_{t-1} + \boldsymbol{b}_h)$$
$$\boldsymbol{h}_t = (1 - \boldsymbol{z}_t) \otimes \boldsymbol{h}_{t-1} + \boldsymbol{z}_t \otimes \tilde{\boldsymbol{h}}_t$$
$$\boldsymbol{o}_t = g(\mathbf{V} \cdot \boldsymbol{h}_t + \boldsymbol{b}_o)$$

**1D-Convolutional Neural Networks**

- Optimized for time-series analysis
- Components: Convolutional, pooling, processing layers
- Feature extraction: Convolutional layers use filters
- Dimensionality reduction: pooling layers emphasize key features
- Flexible processing layer: Options include ANN, RNN, LSTM, GRU
- Efficient in filtering noise from data

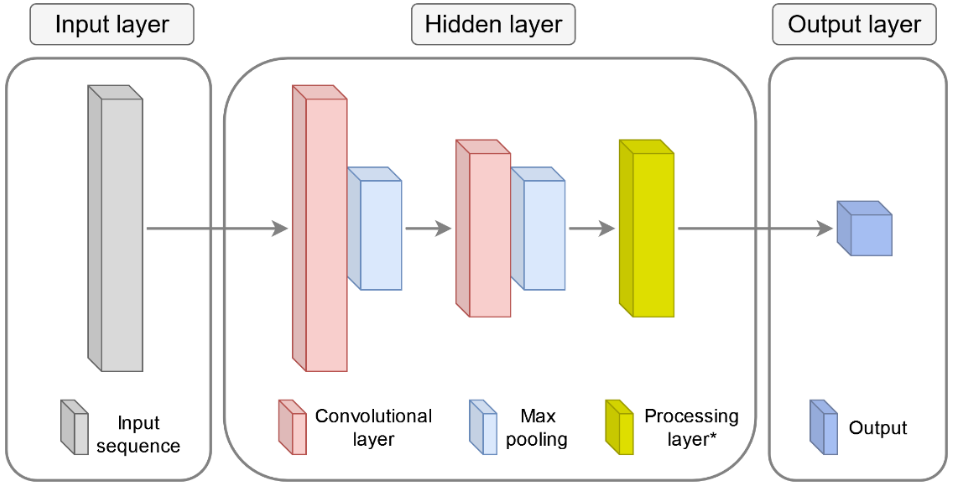

# Methods: DL Models

**Study Evaluated Six DL Models**

- LSTM, GRU, CNN, CNN-LSTM, CNN-GRU, CNN-RNN

**Assessed Across Four Forecasting Lead Times**

- 1 hour, 3 hours, 6 hours, 12 hours

| Lead time (hr) | Model | | | | | |
|---|---|---|---|---|---|---|
| 1 | LSTM | GRU | CNN | CNN-LSTM | CNN-GRU | CNN-RNN |
| 3 | | | | | | |
| 6 | | | | | | |
| 12 | | | | | | |

# Methods: Fit and Uncertainty

**Goodness-of-Fit Evaluation**

- Nash-Sutcliffe Efficiency (NSE): Measures fit between observed and simulated values
- NSE of 1 indicates perfect match
- Weighted NSE (WNSE) accounts for discharge magnitudes
- WNSE Adjusts weights based on observed discharge
- Positive *p* in WNSE emphasizes peak flows
- Negative *p* in WNSE emphasizes low flows

$$NSE = 1 - \frac{\sum_{i=1}^{N}(y^{(i)} - \hat{y}^{(i)})^2}{\sum_{i=1}^{n}(y^{(i)} - \overline{y}^{(i)})^2}$$

$$WNSE = 1 - \frac{\sum_{i=1}^{N} w_i (y^{(i)} - \hat{y}^{(i)})^2}{\sum_{i=1}^{N} w_i (y^{(i)} - \overline{y}_{\mathbf{w}})^2} \qquad w_i = \frac{(y^{(i)})^p}{\sum_{i=1}^{n}(y^{(i)})^p}$$

**Monte Carlo Dropout: Uncertainty Quantification**

- Efficient alternative: No model architecture changes
- Dropout in inference phase
- Process: Random weights set to zero
- Result: Diverse outputs reflect prediction variability
- Method: Average over $T$ stochastic passes
- Output: Estimates predictive mean and variance

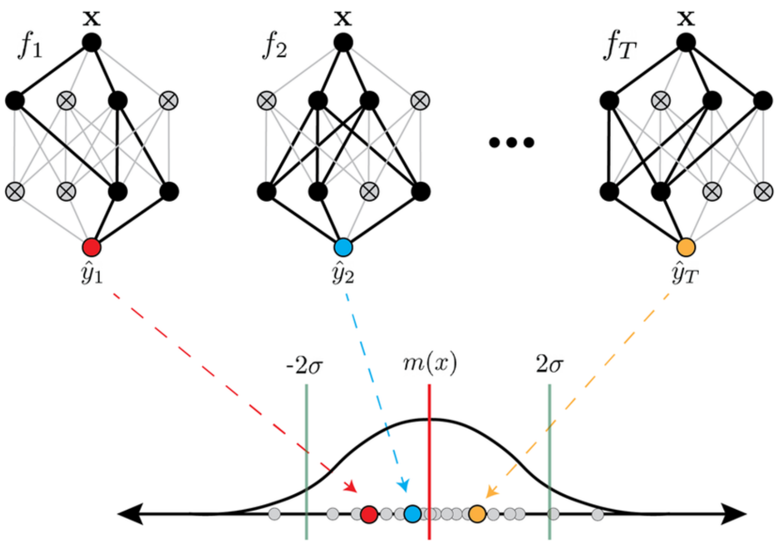

# Methods: Model Inputs

### Input Variable Selection

- Forecasting Q(t) with prior time steps data
- Uses Q(t-1), Q(t-2), R(t-1), R(t-2) as inputs
- Approach minimizes computational demands
- Incremental addition of prior time steps
- Continues until no further improvement in performance

### Model Training

- DL models trained using TensorFlow
- Hyperparameters tuned via trial and Error
- Epochs set to 100
- Data normalized to [0,1] range
- Dropout rate set to 0.10
- Loss function: Mean squared error (MSE)

| Sequence | Input Variables |
|---|---|
| $S_1$ | Q(t-1), R(t-1) |
| $S_2$ | Q(t-1), Q(t-2), R(t-1), R(t-2) |
| $S_3$ | Q(t-1), Q(t-2), Q(t-3), R(t-1), R(t-2), R(t-3) |
| $S_4$ | Q(t-1), Q(t-2), Q(t-3), Q(t-4), R(t-1), R(t-2), R(t-3), R(t-4) |
| ... | ... |
| ... | ... |
| $S_k$ | Q(t-1), Q(t-2), Q(t-3), Q(t-4),..., Q(t-k), R(t-1), R(t-2), R(t-3), R(t-4),..., R(t-k) |

# Results: Training Phase

- **Trend of Increasing Errors with Longer Lead Times**
  - Errors grow as forecast period extends.
  - Likely due to accumulating uncertainties.
- **No Overfitting Observed**
  - Training and validation errors closely aligned.
  - Refer to appendix for detailed scatter plots.
- **Use of MSE as Loss Function**
  - MSE calculated for forecasts between 1 to 12 hours.
- **Performance Variance Between Catchments**
  - Differences due to denormalized data handling.
  - Larger flow rates in Anllóns lead to higher MSE values.
  - Does not indicate less accuracy in Anllóns models.

| Lead time (hr) | Model | MSE $(m^3/s)^2$ Training Groba | MSE $(m^3/s)^2$ Validation Groba | MSE $(m^3/s)^2$ Training Anllóns | MSE $(m^3/s)^2$ Validation Anllóns |
|---|---|---|---|---|---|
| 1 | LSTM | 0.03 | 0.03 | 1.07 | 1.08 |
| 3 | LSTM | 0.09 | 0.08 | 2.71 | 2.77 |
| 6 | LSTM | 0.18 | 0.15 | 4.17 | 4.04 |
| 12 | LSTM | 0.23 | 0.22 | 17.05 | 15.88 |
| 1 | GRU | 0.02 | 0.02 | 0.97 | 0.98 |
| 3 | GRU | 0.09 | 0.07 | 1.94 | 1.96 |
| 6 | GRU | 0.17 | 0.17 | 3.94 | 3.83 |
| 12 | GRU | 0.24 | 0.22 | 16.18 | 15.55 |
| 1 | CNN | 0.03 | 0.03 | 1.07 | 1.08 |
| 3 | CNN | 0.09 | 0.09 | 2.22 | 2.23 |
| 6 | CNN | 0.18 | 0.15 | 4.25 | 4.17 |
| 12 | CNN | 0.22 | 0.21 | 17.81 | 17.09 |
| 1 | CNN-LSTM | 0.03 | 0.03 | 1.26 | 1.18 |
| 3 | CNN-LSTM | 0.09 | 0.09 | 1.91 | 1.88 |
| 6 | CNN-LSTM | 0.18 | 0.15 | 5.69 | 5.58 |
| 12 | CNN-LSTM | 0.24 | 0.22 | 15.17 | 14.31 |
| 1 | CNN-GRU | 0.03 | 0.03 | 1.36 | 1.27 |
| 3 | CNN-GRU | 0.09 | 0.07 | 1.76 | 1.68 |
| 6 | CNN-GRU | 0.18 | 0.14 | 6.08 | 6.05 |
| 12 | CNN-GRU | 0.23 | 0.22 | 16.79 | 16.41 |
| 1 | CNN-RNN | 0.04 | 0.05 | 1.55 | 1.56 |
| 3 | CNN-RNN | 0.09 | 0.08 | 2.12 | 1.92 |
| 6 | CNN-RNN | 0.18 | 0.14 | 4.85 | 4.86 |
| 12 | CNN-RNN | 0.26 | 0.25 | 14.16 | 13.35 |

# Main Results: Testing Phase

**Predictive Skills in Testing Set**

- Data of the training phase is omitted for the sake of conciseness.
- DL models presented similar results with some exceptions
- Groba Basin: GRU models outperform others at 1h
- Anllóns Basin: Consistently high NSE near 0.99 at 1-hour
- Performance generally declines with longer lead times
- Groba Basin shows steep decrease in WNSE high values
- Anllóns Basin maintains better long-term performance
- Hybrid models (CNN-LSTM, GRU) not superior to simple architectures

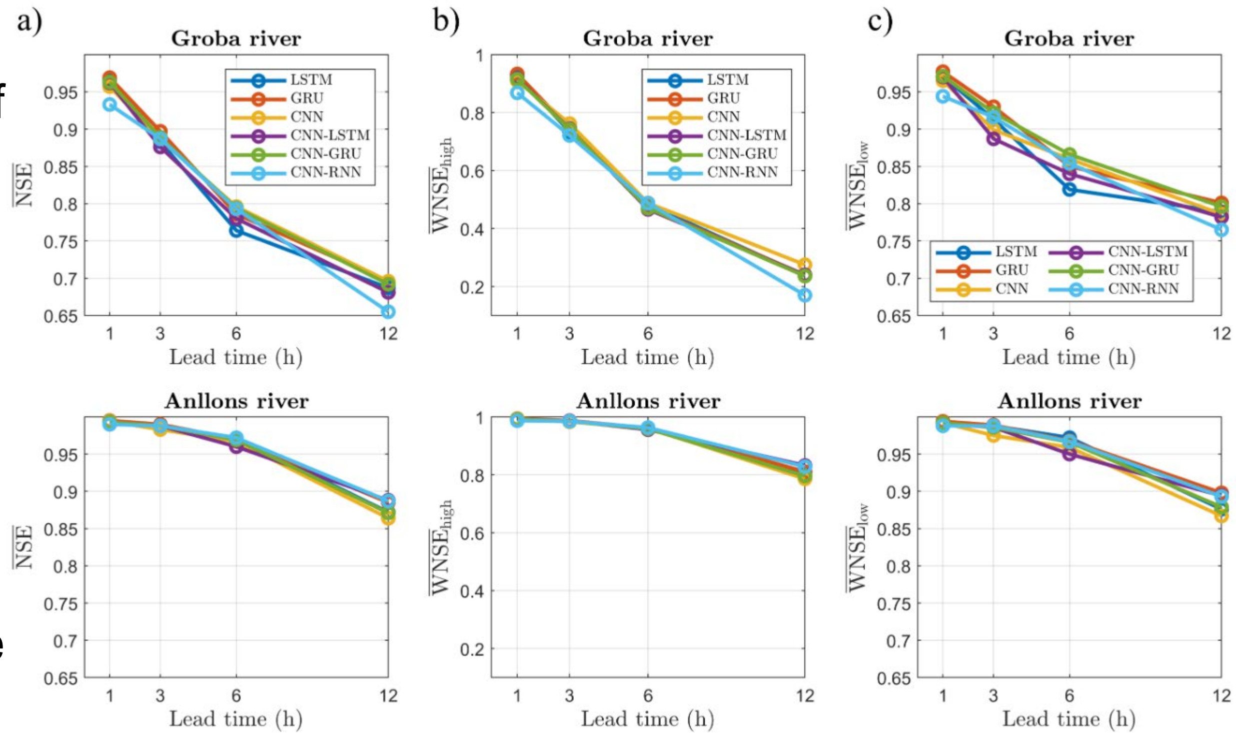

# Main Results: GRU vs. Naive Forecast (Groba basin)

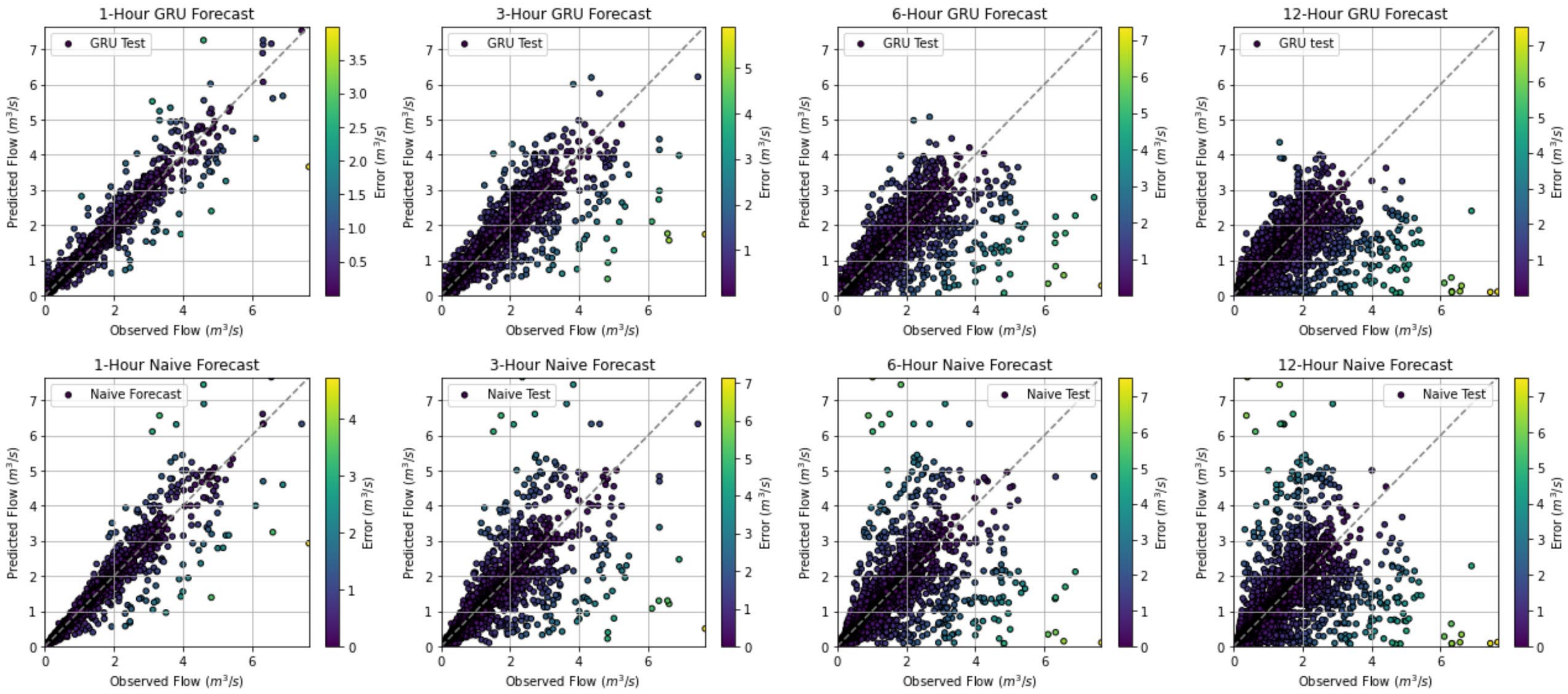

# Main Results: GRU vs. Naive Forecast (Groba basin)

- A naive forecast: Predicts future values based on the most recent data point.
- It predicts the next value will be the same as the last observed value.
- Used as a baseline to assess the performance of more complex forecasting models.

| Groba | | | | | |
|---|---|---|---|---|---|
| GRU | | | | | |
| Time Step | RMSE | MAE | NSE | WNSE-HF | WNSE-LF |
| 1-Hour | 0.110 | 0.031 | 0.969 | 0.933 | 0.977 |
| 3-Hour | 0.202 | 0.055 | 0.897 | 0.746 | 0.930 |
| 6-Hour | 0.290 | 0.099 | 0.786 | 0.474 | 0.850 |
| 12-Hour | 0.347 | 0.095 | 0.696 | 0.240 | 0.801 |
| Naive | | | | | |
| Time Step | RMSE | MAE | NSE | WNSE-HF | WNSE-LF |
| 1-Hour | 0.138 | 0.023 | 0.952 | 0.878 | 0.971 |
| 3-Hour | 0.264 | 0.051 | 0.823 | 0.585 | 0.885 |
| 6-Hour | 0.344 | 0.075 | 0.700 | 0.363 | 0.787 |
| 12-Hour | 0.410 | 0.102 | 0.574 | 0.133 | 0.671 |

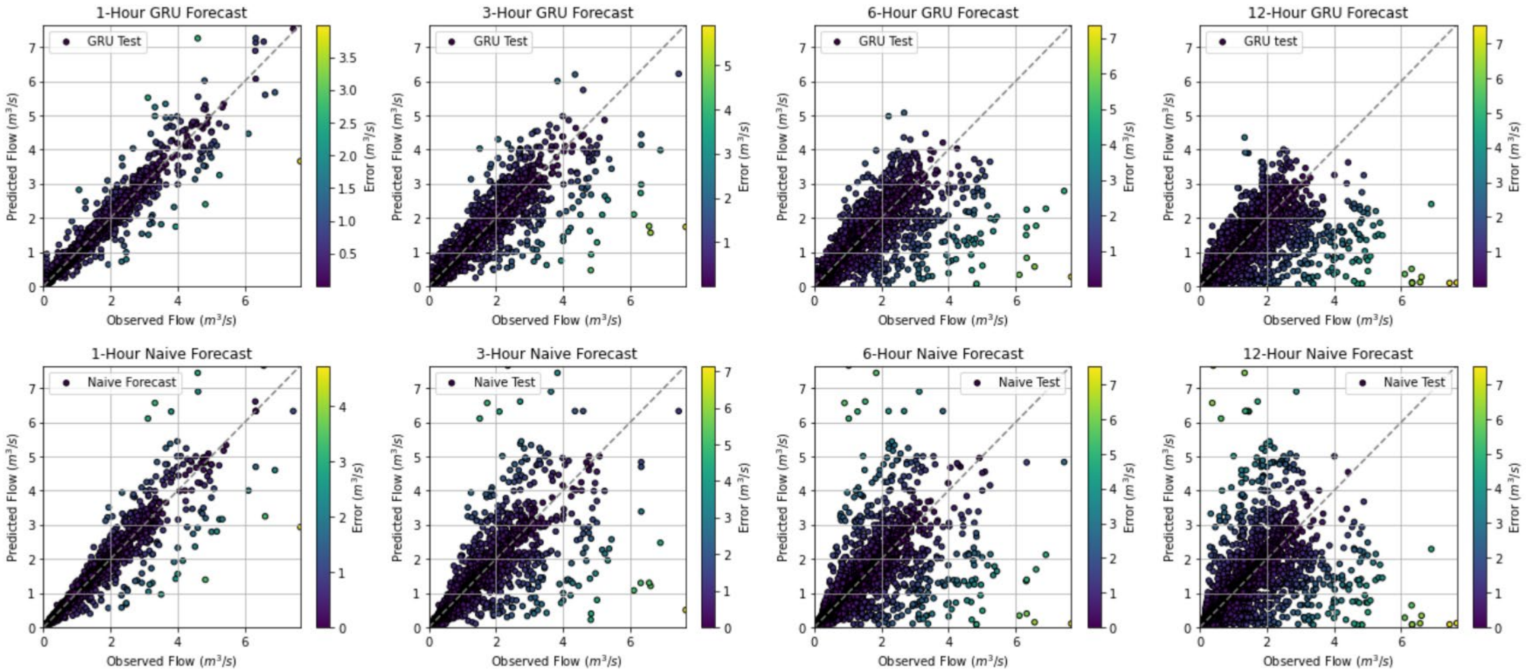

# Main Results: GRU vs. Naive Forecast (Groba basin)

**High and Low Flow Performance (WNSE-HF and WNSE-LF Scores):**

- GRU Model performs better in both high and low flow scenarios compared to the Naive model across all time steps.
- Naive Model consistently lower WNSE-HF, indicating weaker performance in high flow conditions.
- Both models exhibit decreasing performance with increasing lead time, more pronounced in the Naive model.

| Groba | | | | | |
|---|---|---|---|---|---|
| **GRU** | | | | | |
| Time Step | RMSE | MAE | NSE | WNSE-HF | WNSE-LF |
| 1-Hour | 0.110 | 0.031 | 0.969 | 0.933 | 0.977 |
| 3-Hour | 0.202 | 0.055 | 0.897 | 0.746 | 0.930 |
| 6-Hour | 0.290 | 0.099 | 0.786 | 0.474 | 0.850 |
| 12-Hour | 0.347 | 0.095 | 0.696 | 0.240 | 0.801 |
| **Naive** | | | | | |
| Time Step | RMSE | MAE | NSE | WNSE-HF | WNSE-LF |
| 1-Hour | 0.138 | 0.023 | 0.952 | 0.878 | 0.971 |
| 3-Hour | 0.264 | 0.051 | 0.823 | 0.585 | 0.885 |
| 6-Hour | 0.344 | 0.075 | 0.700 | 0.363 | 0.787 |
| 12-Hour | 0.410 | 0.102 | 0.574 | 0.133 | 0.671 |

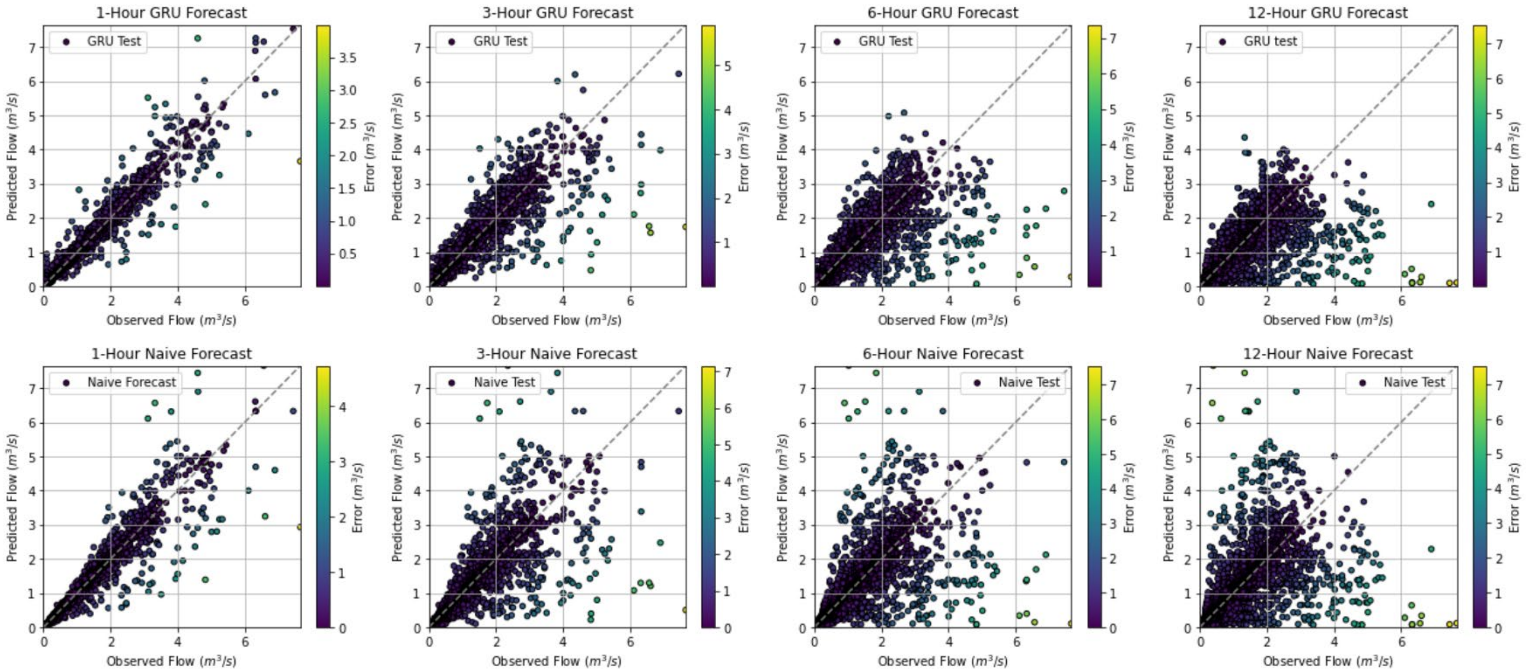

# Main Results: GRU vs. Naive Forecast (Anllóns basin)

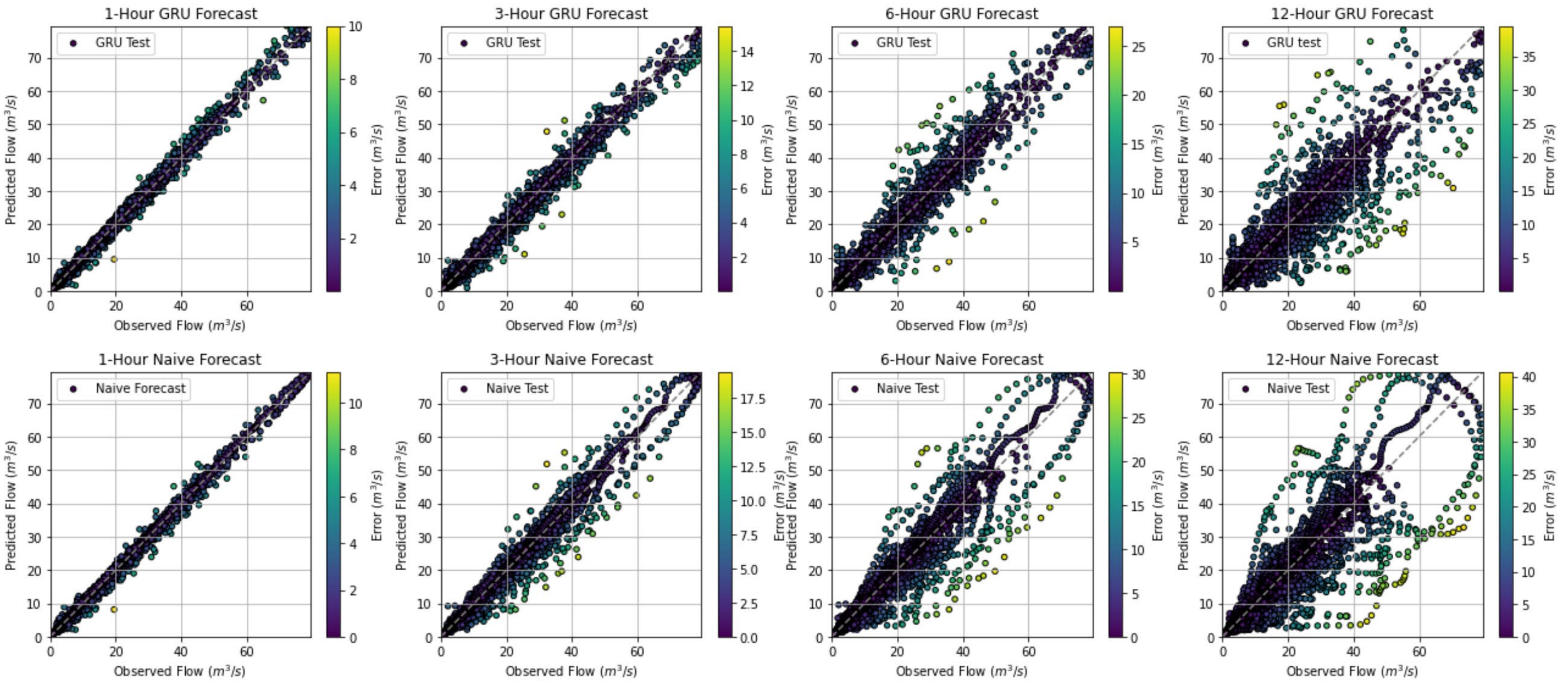

# Main Results: GRU vs. Naive Forecast (Anllóns basin)

- The Naive model performs slightly better across the 1-hour time step.
- This could be due to the lack of significant variation between states in consecutive hours due to the characteristics of the basin.
- The GRU model performs better in 3, 6 and 12-hour lead times.
- The results of the deep learning models are better for lead times close to the time of concentration.

| Anllóns | | | | | |
|---|---|---|---|---|---|
| GRU | | | | | |
| Time Step | RMSE | MAE | NSE | WNSE-HF | WNSE-LF |
| 1-Hour | 0.700 | 0.413 | 0.995 | 0.994 | 0.994 |
| 3-Hour | 1.006 | 0.544 | 0.990 | 0.987 | 0.989 |
| 6-Hour | 1.718 | 0.829 | 0.970 | 0.962 | 0.968 |
| 12-Hour | 3.142 | 1.154 | 0.901 | 0.849 | 0.909 |
| Naive | | | | | |
| Time Step | RMSE | MAE | NSE | WNSE-HF | WNSE-LF |
| 1-Hour | 0.492 | 0.194 | 0.998 | 0.997 | 0.997 |
| 3-Hour | 1.252 | 0.440 | 0.984 | 0.977 | 0.985 |
| 6-Hour | 2.268 | 0.753 | 0.948 | 0.918 | 0.956 |
| 12-Hour | 3.761 | 1.263 | 0.858 | 0.757 | 0.881 |

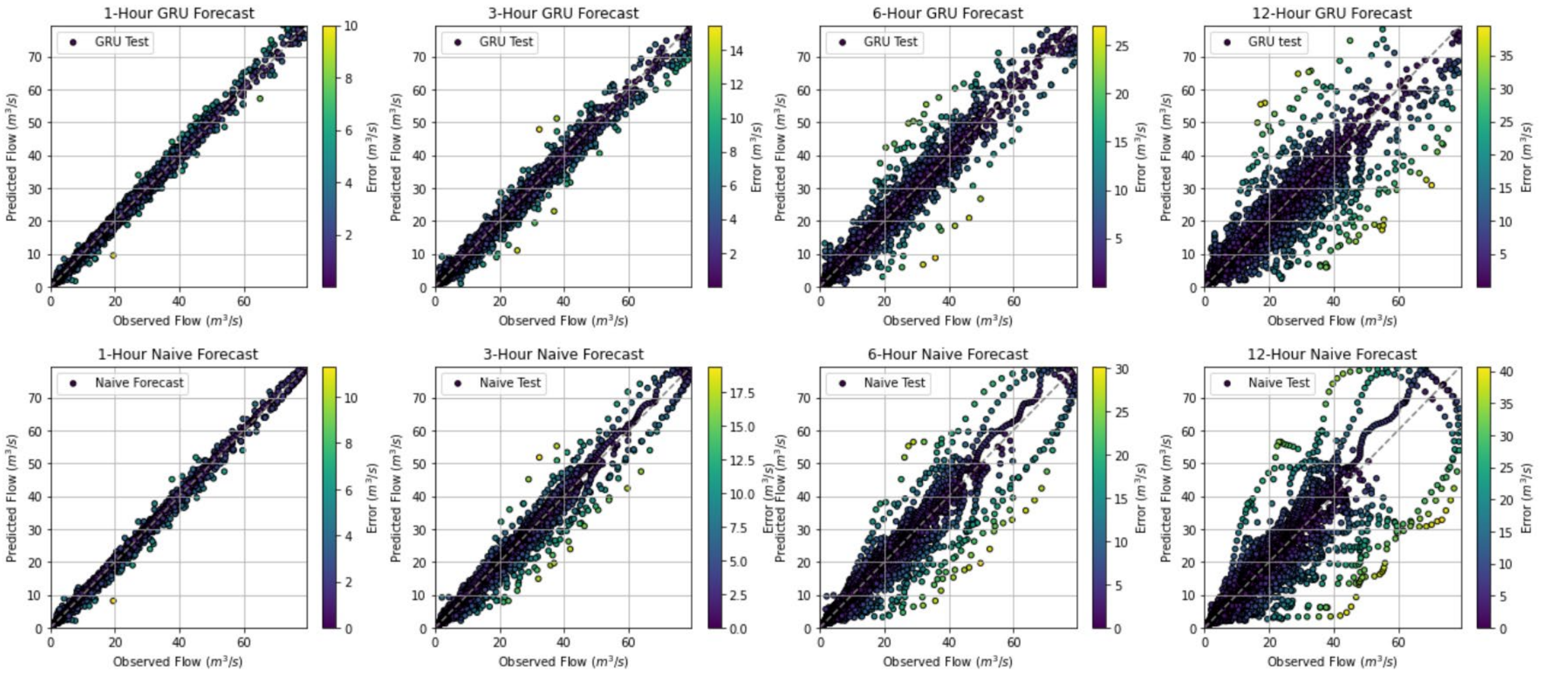

# Discussion

- No single DL model consistently outperforms others across all scenarios.
- Hybrid models (CNN-LSTM, CNN-GRU, CNN-RNN) show no significant advantage over simpler LSTM and GRU models.
- Longer lead times show increased challenges in maintaining accuracy.
- The complexity of hydrological processes affects performance (i.e area and slope).
- Shorter concentration time in basins like Groba limits effectiveness beyond very short lead times.
- In Groba, models fail for lead times longer than 1 hour.
- Models maintain better predictive accuracy in Anllóns basin.
- Adding more historical data does not improve model accuracy for longer lead times.

| Methods | Groba | Anllóns |
|---|---|---|
| | Tc (Hr) | Tc (Hr) |
| Témez | 1.83 | 8.91 |
| Giandoti | 1.47 | 9.93 |

*Times of concentration for the Groba and Anllóns basins using the methods by de Obras Públicas y Urbanismo (1978) and Giandoti Giandotti (1933)*

# Main Results: Isolated Event in Groba Basin

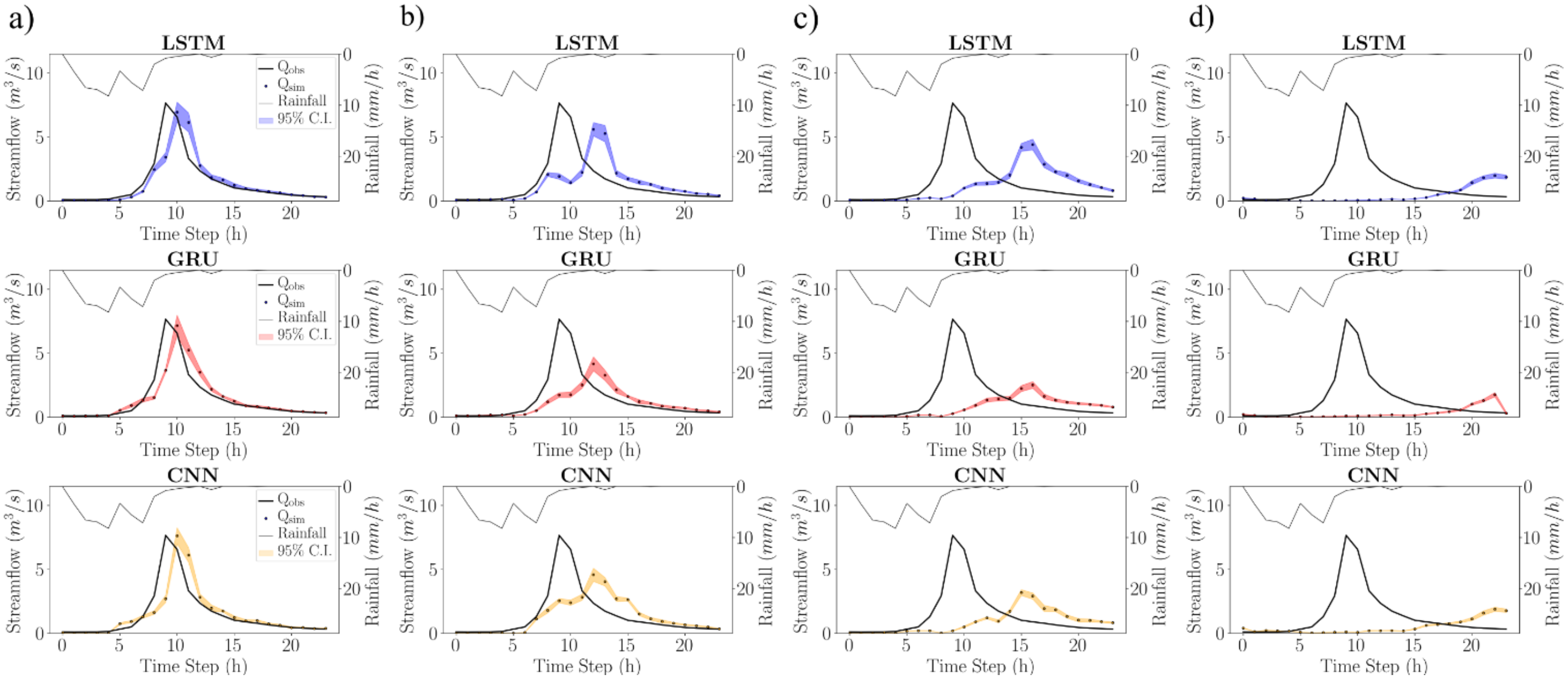


*Visualization of the testing set for the Groba river, featuring observed values, mean forecast, and 95\% confidence intervals at varying lead times: a) 1-hour, b) 3-hours, c) 6-hours, and d) 12-hours. The event data corresponds to November 24, 2017, at 20:00:00.*

# Discussion

- No single DL model consistently outperforms others across all scenarios.
- Hybrid models (CNN-LSTM, CNN-GRU, CNN-RNN) show no significant advantage over simpler LSTM and GRU models.
- Longer lead times show increased challenges in maintaining accuracy.
- The complexity of hydrological processes affects performance (i.e area and slope).
- Shorter concentration time in basins like Groba limits effectiveness beyond very short lead times.
- In Groba, models fail for lead times longer than 1 hour.
- Models maintain better predictive accuracy in Anllóns basin.
- Adding more historical data does not improve model accuracy for longer lead times.

| Methods | Groba | Anllóns |
|---|---|---|
| | Tc (Hr) | Tc (Hr) |
| **Témez** | 1.83 | 8.91 |
| **Giandoti** | 1.47 | 9.93 |

*Times of concentration for the Groba and Anllóns basins using the methods by de Obras Públicas y Urbanismo (1978) and Giandoti Giandotti (1933)*

# Main Results: : Isolated Event in Anllóns Basin

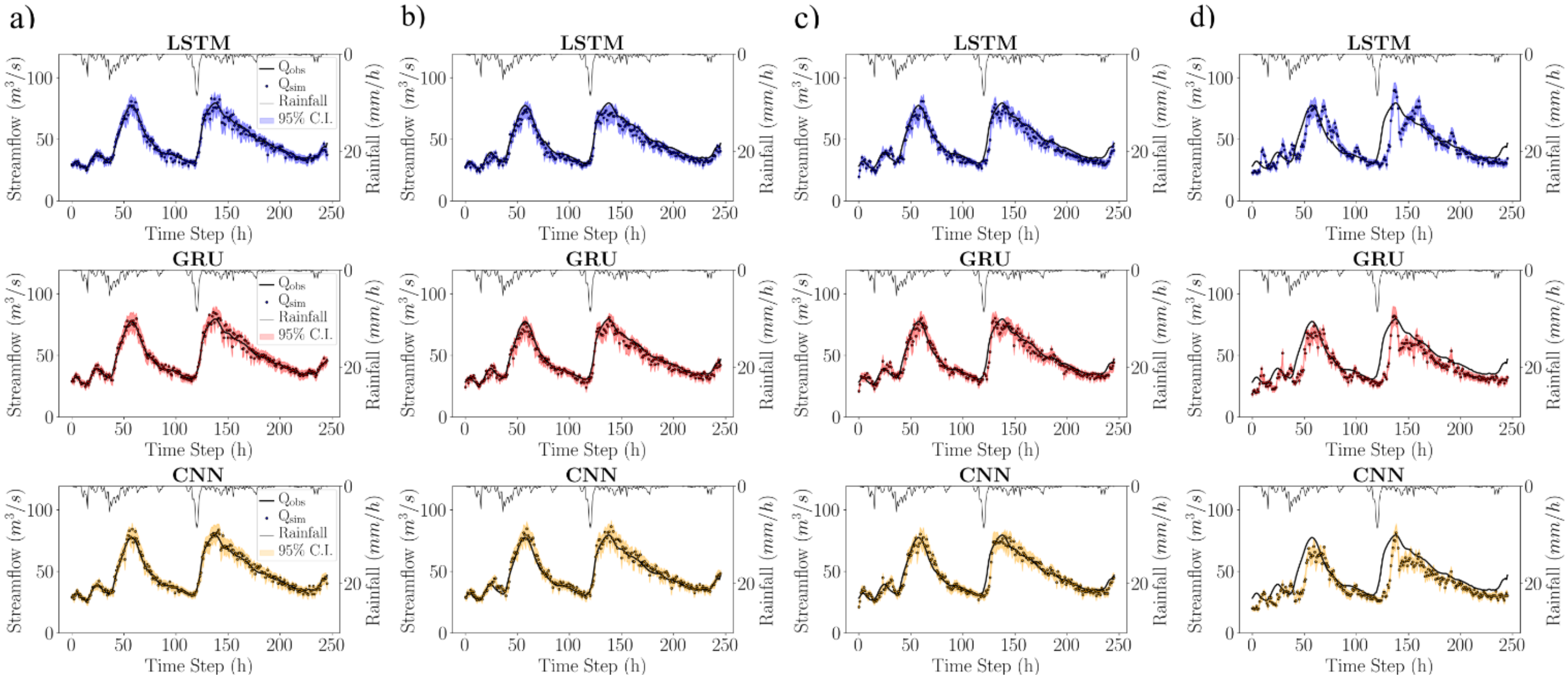


*Visualization of the testing set for the Anllóns river, featuring observed values, mean forecast, and 95\% confidence intervals at varying lead times: a) 1-hour, b) 3-hours, c) 6-hours, and d) 12-hours. The data for the two events are from March 13, 2018, at 21:00:00 and March 15, 2018, at 03:00:00.*

# Conclusions

- Six DL Models were Evaluated in Two Spanish Basins.
- No Single Model Dominated Across All Conditions.
- Hybrid Models Like CNN-LSTM Showed No Clear Advantage.
- Significant Accuracy Drop Over Longer Lead Times in Small Basins.
- Performance Affected by Hydrological Basin Characteristics (Time of Concentration).
- Different Data Sources can Improve Extend the Presented Application.
- Incorporating Rainfall Forecasts May Extend Lead Times.
- This Study is a First Approximation in our Study Region.
- Provides Baseline for Future DL Model Applications.

# OPTIMIZATION OF DISTRIBUTED MODELS USING EVOLUTIONARY ALGORITHMS AND SURROGATE MODELING

Juan F. Farfán-Durán[1], Arash Heidari[2], Ivo Couckuyt[2], Tom Dhaene[2], Jerónimo Puertas[1], Luís Cea[1]

1 *Universidade da Coruna, Water and Environmental* Engineering *Group, Center for Technological Innovation in Construction and Civil Engineering (CITEEC)*

2 [2] *Faculty of Engineering and Architecture, Ghent University - imec, Ghent, Belgium*

# Basic idea:

- Distributed models based on 2D Shallow Water Equations (SWE) are becoming fundamental in water resources engineering.
- Unstructured mesh (basin area: 240 $Km^2$)
- Running the model hundreds of times, requires a significant investment of computational time.
- Combine a Surrogate Model based on Artificial Neural Networks (SM-ANN) and an Evolutionary Algorithm (EA).
- **Purpose:** To perform the calibration process of a Distributed Model.

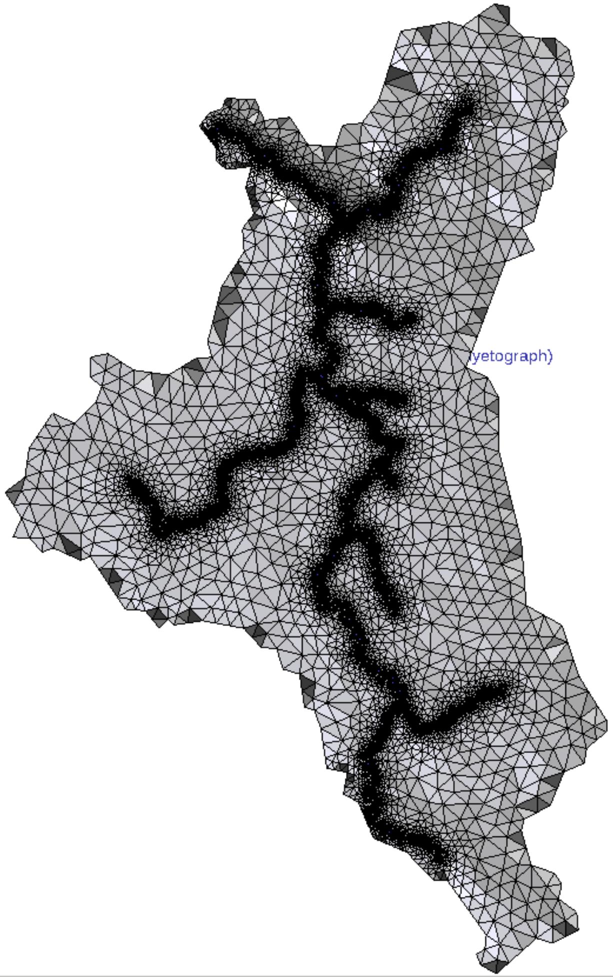

# Structure of the SM-ANN

- **Input:** $\mathbf{X} \in \mathbb{R}^{Nxm_x}$: Individuals in the population. In this case, parameters of the model.
- **Output:** $\mathbf{Y} \in \mathbb{R}^{Nxm_y}$: Fitness of the population members. Objective functions to optimize.
- 2 objective functions: NSE and WNSE
- For a parameter set $\mathbf{x}^{(i)}$, the ANN aims to predict the fitness values $\mathbf{y}*^{(i)}$
- The ANN, creates a simulated solution space.

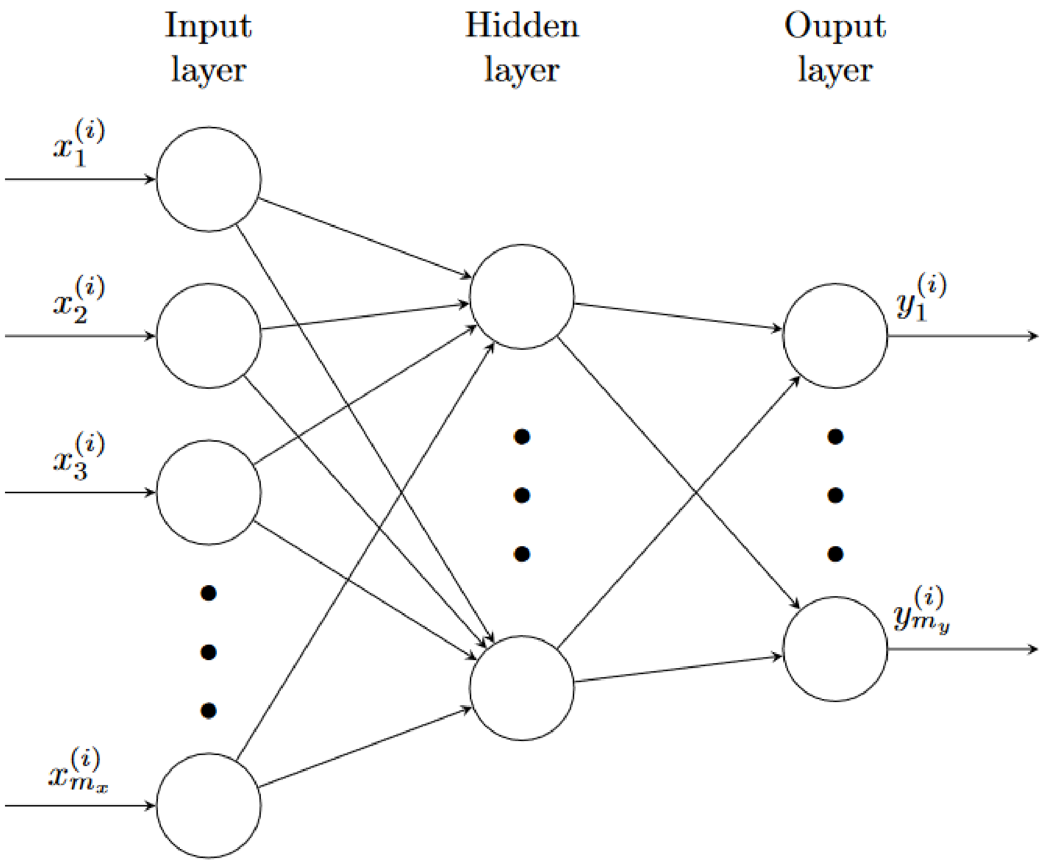

# Scheme of application of the SA-EA

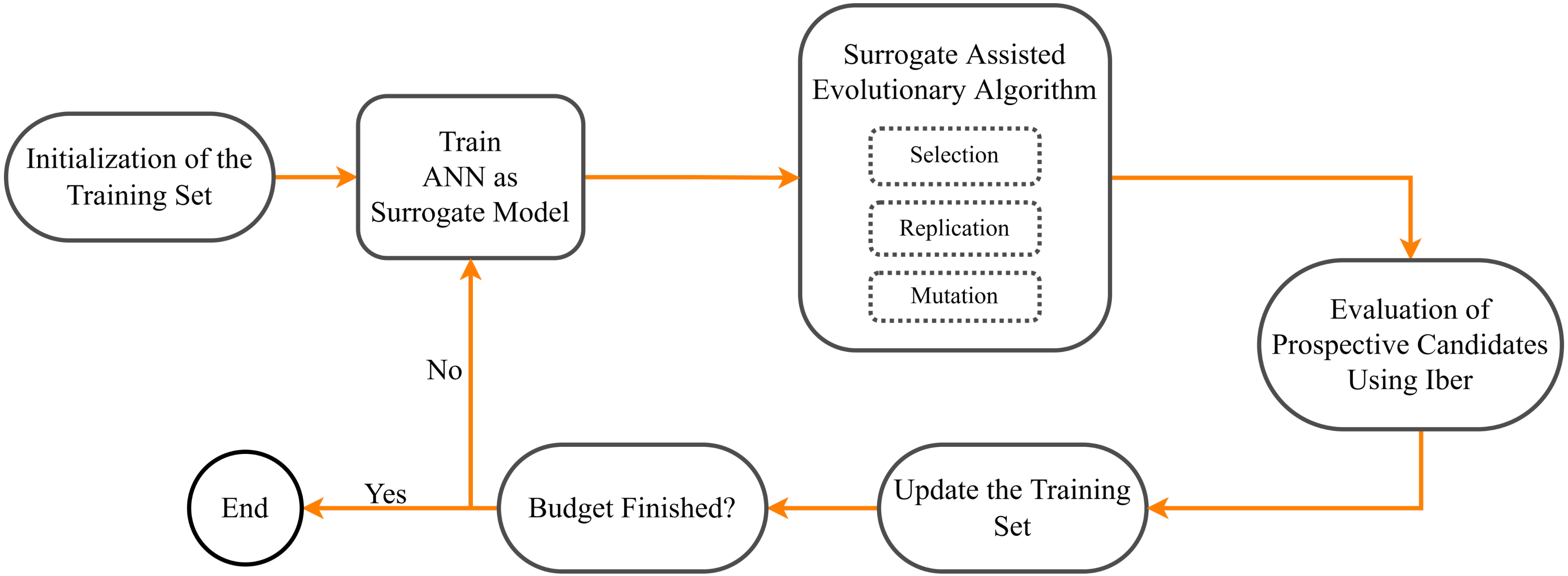

# Real vs. predicted fit values

## a) Synthetic event

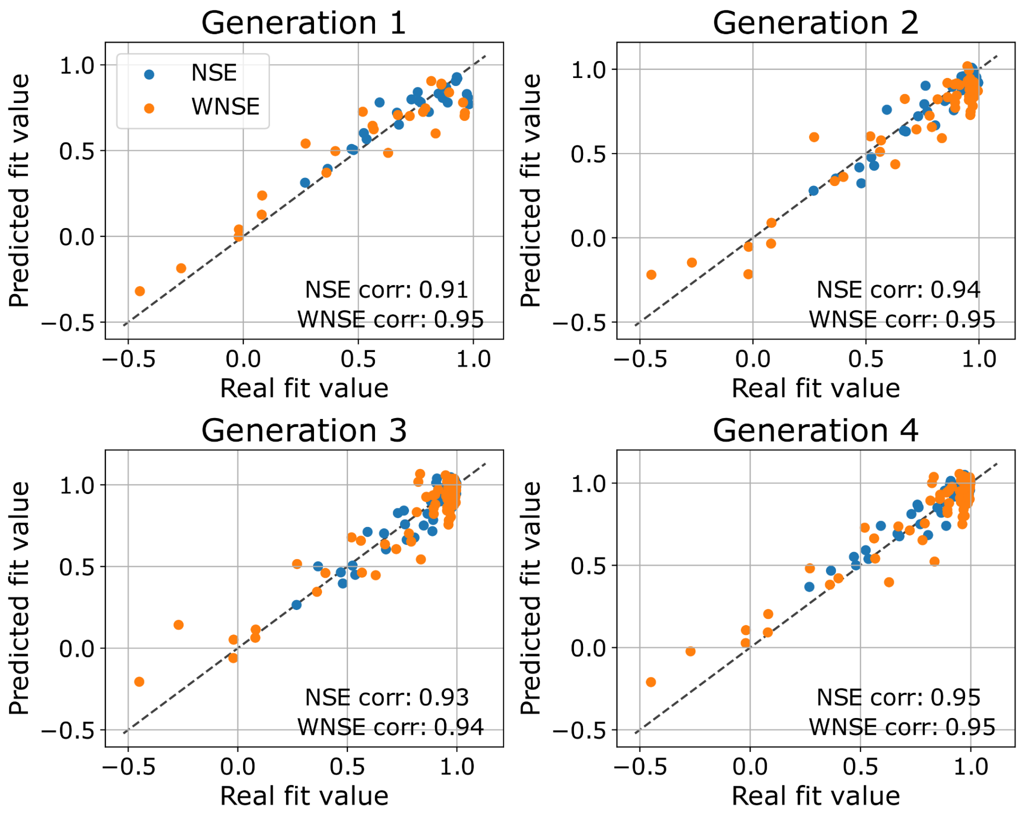


## b) Real event

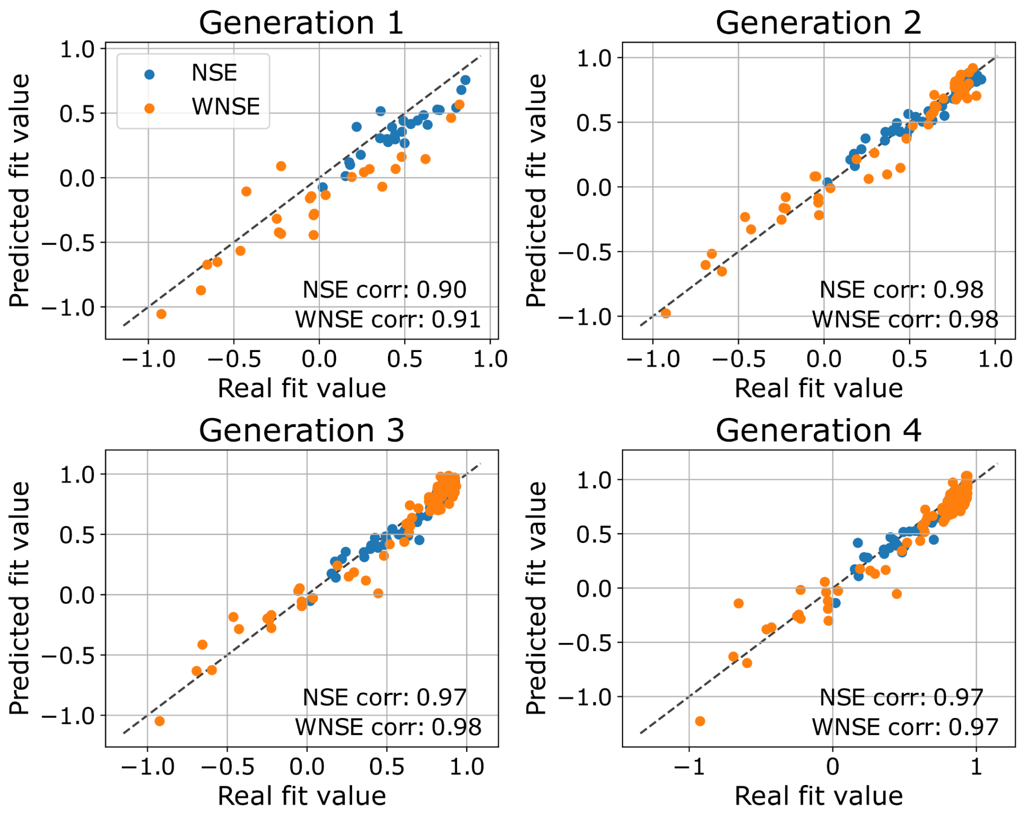

# Observed and simulated hydrographs

a) Synthetic event

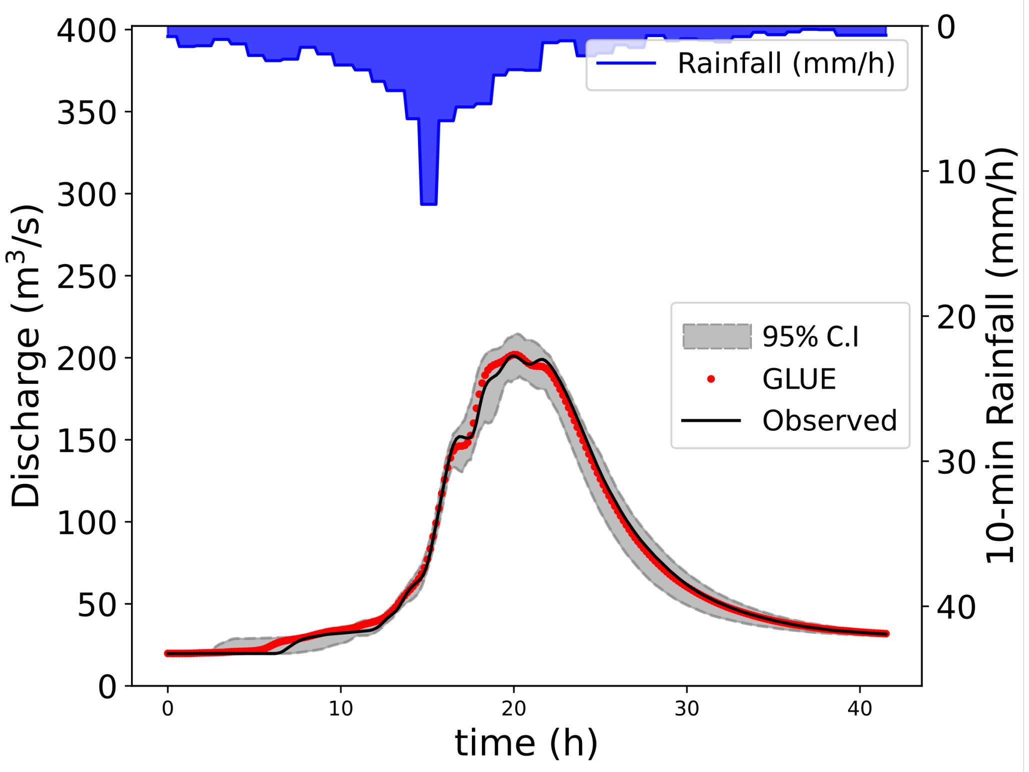


b) Real event

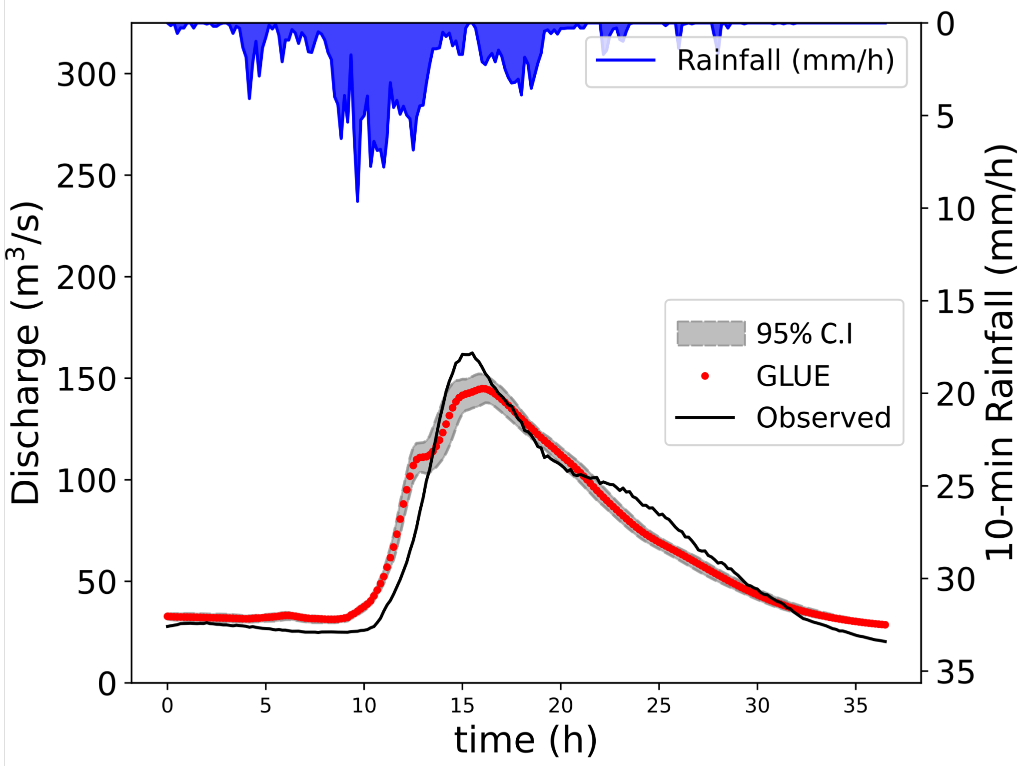

# Computation times

a) Synthetic event

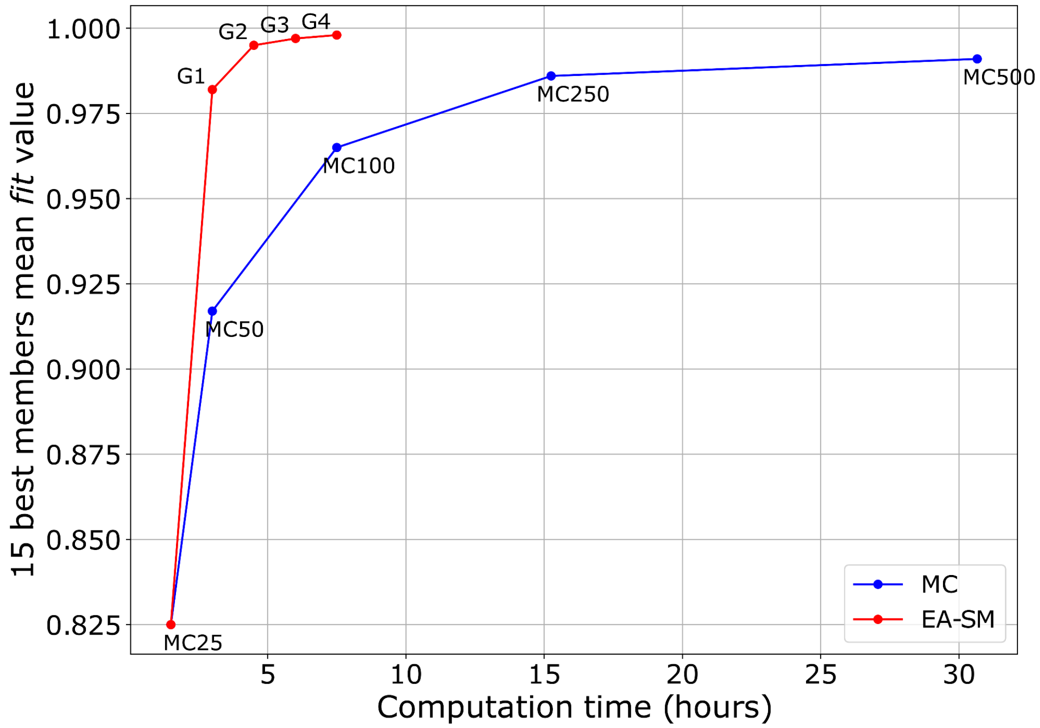


b) Real event

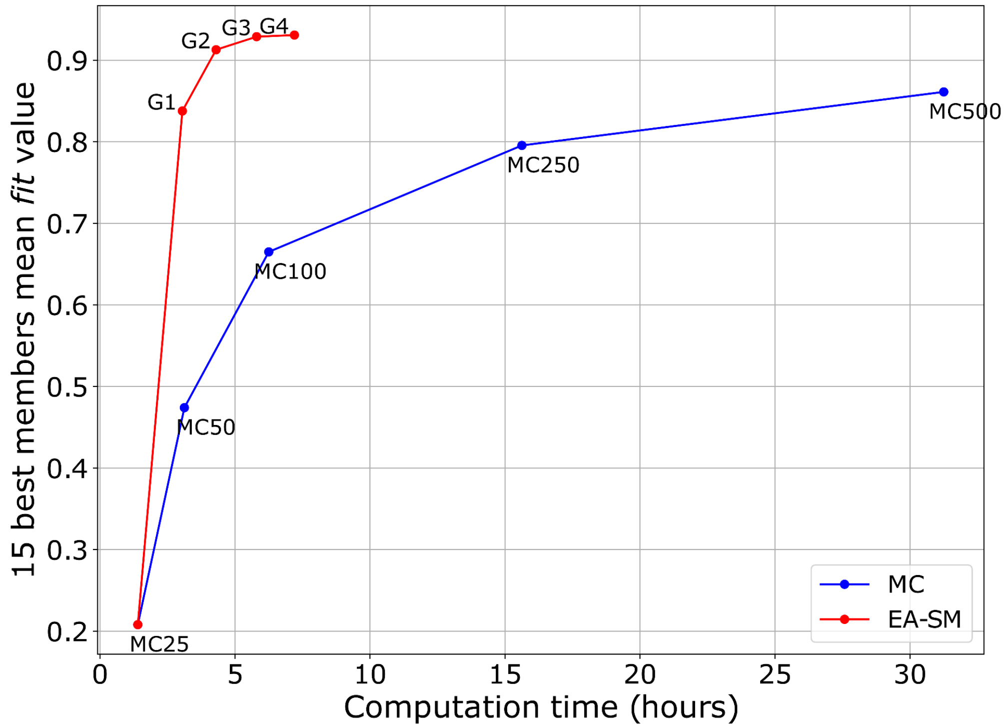

# Bibliography


- Farfán, J. F., & Cea, L. (2021). Coupling artificial neural networks with the artificial bee colony algorithm for global calibration of hydrological models. *Neural Computing and Applications*, *33*, 8479-8494.
- Cea, L., & Bladé, E. (2015). A simple and efficient unstructured finite volume scheme for solving the shallow water equations in overland flow applications. *Water resources research*, *51*(7), 5464-5486.
- Couckuyt, I., Gorissen, D., Rouhani, H., Laermans, E., & Dhaene, T. (2009). Evolutionary regression modeling with active learning: An application to rainfall runoff modeling. In *Adaptive and Natural Computing Algorithms: 9th International Conference, ICANNGA 2009, Kuopio, Finland, April 23-25, 2009, Revised Selected Papers 9* (pp. 548-558). Springer Berlin Heidelberg.

# Thank you

*This work was partially funded by the Spanish Ministry of Science and Innovation (MCIN/AEI/10.13039/501100011033) within the project "SATURNO: Early warning against pluvial flooding in urban areas" (PID2020-118368RB-I00).*

Proyecto SATURNO (PID2020-118368RB-I00)
Sistemas de Alerta Temprana frente a inundaciones pluviales en entornos urbanos
Financiado por el Ministerio de Ciencia e Innovación

GOBIERNO DE ESPAÑA
MINISTERIO DE CIENCIA E INNOVACIÓN

AGENCIA ESTATAL DE INVESTIGACIÓN